Water Resources Research

RESEARCH ARTICLE
10.1029/2024WR039078

Special Collection:
Integrating In Situ, Remote Sensing, And Physically Based Modeling Approaches to Understand Global Freshwater Ice Dynamics

Freeze-Up Ice Jams and Channel Hydraulics Cause Hazardous Open Water Zones Within Winter Ice Cover on the Kuskokwim and Yukon Rivers and Their Tributaries

Christopher D. Arp[1], Dana N. Brown[2], Allen C. Bondurant[1], Karin L. Bodony[3], Melanie Engram[1], Katie V. Spellman[2], Sarah J. Clement[2], and Matthew C. Scragg[1]

[1]Water and Environmental Research Center, University of Alaska Fairbanks, Fairbanks, AK, USA, [2]International Arctic Research Center, University of Alaska Fairbanks, Fairbanks, AK, USA, [3]Koyukuk Nowitna Innoko National Wildlife Refuge Complex, U.S. Fish and Wildlife Service, Galena, AK, USA

Abstract Timing and completeness of freeze-up on northern rivers impact winter travel and indicate responses to climate change. Open-water zones (OWZs) within ice-covered rivers are hazardous and may be increasing in extent and persistence. To better understand the distribution, variability, and mechanisms of OWZs, we selected nine reaches totaling 380 river-km for remote sensing analysis and field studies in western Alaska. We initially identified 48 OWZs from November 2022 optical imagery, inventoried their persistence into late winter and interannual consistency over previous years, and at a subset measured ice thickness, water depth and velocity, and physicochemistry. The most consistent locations of OWZ formation occurred below sharp bends and channel constrictions, whereas locations associated with river bars and eroding banks were more transient. Of 359 OWZs identified in early winter over 6 years, 8% persisted into late winter——all on the Yukon River mainstem. Although several OWZs were in locations where we anticipated groundwater influence, we found no field data indication of groundwater upwelling. Observations of jumble ice upstream of many OWZs led us to examine freeze-up ice jam locations in optical imagery, which showed strong correspondence to downstream OWZs. We hypothesize that reaches downstream of ice jams are much slower to freeze-over due to restricted ice transport and high turbulence caused by channel form and ice-affected hydraulics. Future work should focus on evaluation of this and other competing hypothesis at both reach and river network scales to predict OWZ locations and occurrence relative to other processes affecting river freeze-up in northern climates.

Plain Language Summary Northern rivers traditionally freeze over with complete ice cover and thus serve as important travel and transportation corridors. Incomplete freeze-up in the form of open leads or open-water zones present hazards to winter travelers, yet knowing where, when, and why these hazards form is uncertain. Using a combination of field measurements and satellite observations, we studied hundreds of open-water zone locations on larger rivers and their tributaries in western Alaska over 6 years. Results show that locations where large persistent open-water zones form regularly are associated with narrow valleys and sharp meanders. Deeper channels, higher under-ice flow, and limited groundwater upwelling are also associated with open-water zone locations. Observations during the early freeze-up period suggest that upstream ice jams are the primary cause of open-water zone formation downstream. These ice jams are also hypothesized to enhance turbulence and slow open-water closure. Future research should focus on how freeze-up progresses in warmer winters with higher river flows.

Key Points:

- Incomplete river freeze-up in the form of open-water zones present hazards in a changing climate
- Open-water zones most consistently occur at or below steep hillsides, sharp meanders, and channel constrictions
- Ice jams are hypothesized to cause open-water zones to form downstream due to interrupted ice transport and enhanced turbulence

Supporting Information:

Supporting Information may be found in the online version of this article.

Correspondence to:

C. D. Arp,
cdarp@alaska.edu

Citation:

Arp, C. D., Brown, D. N., Bondurant, A. C., Bodony, K. L., Engram, M., Spellman, K. V., et al. (2025). Freeze-up ice jams and channel hydraulics cause hazardous open water zones within winter ice cover on the Kuskokwim and Yukon rivers and their tributaries. *Water Resources Research*, *61*, e2024WR039078. https://doi.org/10.1029/2024WR039078

Received 30 SEP 2024
Accepted 8 APR 2025

Author Contributions:

Conceptualization: Christopher D. Arp, Dana N. Brown, Allen C. Bondurant
Data curation: Christopher D. Arp, Allen C. Bondurant
Formal analysis: Christopher D. Arp, Dana N. Brown, Allen C. Bondurant, Karin L. Bodony, Melanie Engram, Sarah J. Clement
Funding acquisition: Christopher D. Arp

1. Introduction

Rivers serve as important transportation corridors, particularly in sparsely populated regions like Alaska that lack road networks. In such regions with distinct warm and cold seasons, travel is traditionally by boat and barge in the summer and by snowmachines and sled dogs in the winter, as well as wheeled vehicles on ice roads constructed on larger rivers (Brown et al., 2018; Herman-Mercer et al., 2011; Schneider et al., 2015). Thus the period during freeze-up and break-up is most disruptive to reliable transportation, particularly if the timing of these periods is uncertain and the duration of these periods is getting longer (Brown et al., 2023; Jones et al., 2015; Wilson et al., 2015). Open water zones (also known as open leads or polynyas (International Association for Hydraulic Research Association, 1980)) in otherwise ice-covered rivers represent a form of incomplete freeze-up and present serious risks to river users. The timing and duration of ice cover on northern rivers is also seen as an important indicator of changing climate (Magnuson et al., 2000; Prowse et al., 2011). Beyond creating hazards for

Investigation: Christopher D. Arp, Allen C. Bondurant, Karin L. Bodony, Katie V. Spellman, Sarah J. Clement, Matthew C. Scragg
Methodology: Christopher D. Arp, Dana N. Brown, Allen C. Bondurant, Melanie Engram, Sarah J. Clement, Matthew C. Scragg
Project administration: Christopher D. Arp, Dana N. Brown
Resources: Christopher D. Arp, Karin L. Bodony, Katie V. Spellman
Supervision: Christopher D. Arp
Validation: Christopher D. Arp, Dana N. Brown
Visualization: Katie V. Spellman
Writing – original draft: Christopher D. Arp, Dana N. Brown, Allen C. Bondurant, Karin L. Bodony, Melanie Engram, Katie V. Spellman, Sarah J. Clement, Matthew C. Scragg
Writing – review & editing: Christopher D. Arp, Dana N. Brown

people, these changes have implications for fluvial geomorphology, sediment and biogeochemical transport (C. Arp et al., 2024, C. D. Arp et al., 2024), and riverine habitat (Beltaos & Prowse, 2009; Burrell et al., 2021). Global multi-temporal analyses confirm later river freeze-up, earlier break-up, and shorter overall duration of ice cover (e.g., Magnuson et al., 2000; Yang et al., 2020) and regional Alaska studies elucidate how and why such river-ice changes progress sequentially and impact local travel and subsistence activities (Brown et al., 2018, 2023).

The majority of river-ice research has focused on the break-up period because of hazards caused by ice-jam flooding, while the freeze-up period has seen less attention (Burrell et al., 2021). Physics-based and conceptual models of river freeze-up both describe a sequence of border- and frazil-ice formation, frazil ice-pan growth and transport, and eventual development of a complete ice-cover by a combination of border-ice expansion and ice-pan arresting and lodgment (i.e., jamming) and upstream accumulation (i.e., juxtapositioning) (Blackburn & She, 2019; Brown et al., 2018; Shen, 2010). Freeze-up ice jams form when drifting frazil-ice pans and rafts come to a halt where they freeze together to form a consolidated or juxtaposed ice cover (Bergeron et al., 2011), while break-up ice jams results from a decaying and hydraulically fractured ice cover during rising river levels that mobilize and then lodge or jam downstream (Beltaos & Prowse, 2009). River ice freeze-up processes can vary greatly by channel size, gradient, and complexity (e.g., meandering, anastomosing, and braiding), river discharge and stream power, and climate setting (Bergeron et al., 2011; Brown et al., 2023; Turcotte & Morse, 2013). For example, border ice forms thermally in slow moving water and frazil ice forms most readily in turbulent open-waters during very cold periods ($<-20°C$) (Osterkamp & Gosink, 1983; Shen, 2010). In terms of transferring process understanding to prediction, most river ice models are unable to represent reach-scale heterogeneity in ice-cover formation that would help predict the location and persistence of late freezing open-water zones (OWZs) (Blackburn & She, 2019; Morales-Marín et al., 2019). An important contribution to the conceptual understanding of river ice formation proposed by Bergeron et al. (2011) is based on the river sediment-link concept from fluvial geomorphology (e.g., Rice & Church, 1998) and observations from rivers in southeastern Canada. This model describes sequential variation in ice formation processes along downstream continua that can be disrupted or reset by tributaries, sediment supply, or other fluvial discontinuities (e.g., bedrock canyons, dams). Coupled with the longstanding observations and knowledge of freeze-up ice cover development and corresponding telescoping of lodgment ice-pans upstream of ice-jam points, the Bergeron et al. (2011) river-ice model provides a conceptual basis for understanding and predicting OWZs throughout river networks according to ice formation and transport interaction with channel morphology and hydraulics. To our knowledge, this model has not yet been applied to higher latitude rivers systems like in western Alaska.

Alternative hypotheses concerning the location and persistence of OWZs come from both coarse- and fine-scale observations of river ice behavior in the context of regional watershed dynamics (Jones et al., 2015). The relationship between air temperature and freeze-up timing is generally well established (e.g., Beltaos & Prowse, 2009; Osterkamp & Gosink, 1983) with recent time-series observations of river ice-cover duration linked to air temperature at a global-scale (e.g., Yang et al., 2020) and at river-basin scales (e.g., Brown et al., 2018, 2023). Other factors, such as autumn and early winter river discharge, are often considered to cause additional variability in freeze-up timing because more water and associated higher water-levels and velocities should equate to delayed ice-cover formation (Beltaos, 2013; Beltaos & Prowse, 2009; Burrell et al., 2021). Observed increases in winter flows of northern rivers, such as the Yukon, are often attributed to shrinking permafrost distribution and resulting enhanced groundwater-flux augmenting winter baseflow (Bennett et al., 2023; Walvoord & Kurylyk, 2016; Walvoord & Striegl, 2007). In addition to more and perhaps warmer water slowing ice formation, there is a recurrent suggestion that new and stronger groundwater upwelling zones are causing new and persistent OWZs in many northern rivers (e.g., Herman-Mercer et al., 2011; Saros et al., 2022; Schneider et al., 2015; Wilson et al., 2015). Detailed field observations and modeling by Jones et al. (2015) on the Tanana River in Alaska examined the role of groundwater upwelling in maintaining OWZs on backwater sloughs, however they found flow velocities to be a more important factor. Observations of OWZs in other streams and small rivers with strong groundwater contributions are also commonly reported (Clawson et al., 2022; Jones et al., 2015) and in many cases may be linked to local or regional permafrost degradation or just as often persistent springs and seeps associated with local or regional geology (Osterkamp & Gosink, 1983). The occurrence of persistent OWZs on larger northern rivers, however, may relate more directly to how ice-cover forms along channel flowpaths with heterogeneous velocities that impact frazil- and pan-ice production and transport (Brown et al., 2023; Burrell et al., 2021; Das et al., 2015). The interaction between higher winter discharge and river

geomorphology coupled with mechanisms of ice formation and transport may help explain observations of persistent OWZ in many river systems.

In the case of medium-to-large northern river systems (>100-m width), which are the predominant routes utilized for winter travel and the focus of this study in western Alaska, we are working to better understand the freeze-up process as it relates to OWZ hazards. Context for this study focuses on broad hypotheses related to changes in climate, permafrost, discharge, and groundwater (Jones et al., 2015; Saros et al., 2022) compared to interactions between ice formation, transport, and complete freeze-up along a river continuum (Bergeron et al., 2011). Our goal is to improve understanding of where, when, and why OWZs develop and persist in otherwise contiguous ice cover in order to facilitate more reliable prediction, as well as more nuanced attribution of these winter hazards. Using a combination of remote sensing and field studies, our objectives were to (a) characterize the extent, seasonal persistence, and interannual consistency of OWZs, (b) determine the relative roles of hydroclimatic and hydrogeomorphic controls on OWZ location, size, and persistence, and (c) advance understanding of the mechanisms causing OWZs to form and persist.

2. Methods

2.1. Study Area and Design

Selection of our nine study reaches was initially based on proximity to the villages of McGrath, Shageluk, and Galena, which we visited for science education and outreach and our associated travel route between these communities along the Iditarod Trail (Figure 1). The presence of OWZs along this route presented a potential hazard for our research team, just as it does for residents of these and many other towns and villages along rivers in western Alaska, but also presented an important opportunity to observe and study them. Thus study reaches on the Yukon and Kuskokwim rivers, the two largest rivers in Alaska, and their tributaries, directly coincided with our field travel route in March 2023 and the interests of communities we were visiting. Reach extents generally scaled with river size, averaging 42 km in length (Table 1). The smallest reach, situated on the Iditarod River, was 15 km long with an average channel width of 50 m. The largest was the lowest study reach of the Yukon River near Anvik, extending 60 km with an average channel width of 1,400 m. The form of all study reaches of the Yukon River was classified as anastomosing and other study reaches were classified as meandering (Table 1).

Prior to March 2023 fieldwork, we identified 48 OWZs large enough to accurately observe with moderate resolution satellite imagery (10-m resolution Sentinel 2 or 30-m resolution Landsat 8) acquired in late November 2022. Based on this initial inventory, we selected 23 OWZ locations to visit in the field primarily according to reasonable deviations in our intended travel route. Exact locations for field data collection were based on standard positions relative to individual late-freezing OWZs. The upstream heads of OWZs were generally assumed to freeze last (OWZ-H), typically in December or later, downstream tails of OWZ were assumed to freeze earlier (OWZ-T), and locations adjacent to OWZs were known to have ice cover at the time of image acquisition and thus froze earliest (REF, Figures 2c, 2f, 2i and 2l). By selecting sampling locations relative to known early winter OWZ locations in the season of our field studies, this allowed us to differentiate and make general inferences about ice formation timing and processes that were consistent among sites, river reaches, and river systems.

2.2. Remote Sensing Detection

Initial identification of OWZs was conducted by searching archives in Planet Explorer (Planet Labs PBC, 2023) for available cloud-free satellite images during the 2022 freeze-up period until approximately early December when low-light and sun-angles prohibit passive optical satellite imaging at the latitude of our study area. We were able to acquire Landsat 8 images at 30-m resolution covering the Kuskokwim and Takotna rivers for 29-Nov, the Yukon River at Anvik and Innoko River for 26-Nov, and the other Yukon River reaches and the Koyukuk River for 20-Nov. For this same year on the Iditarod River, we acquired Sentinel-2B images at 10-m resolution for 15-Nov. We also acquired cloud-free summer images for the same study reaches during a period of low water to aid in OWZ differentiation from channel islands and bars, which were all from Sentinel-2A on 10-June 2022 (examples in Figures 2a, 2d, 2g and 2j). All images were downloaded as RGB GeoTiffs optimized for visual analysis and brought into ArcMap 10.8 for further analysis. All OWZs larger than 2 pixels or 60 m in Landsat 8 imagery (median OWZ length was much larger, 18 pixels or 520 m) were identifiable as dark zones (usually black) set within white, typically snow-covered river-ice, which could be distinguished from channel bars and islands and from shadows cast from shoreline topography and trees. All OWZs were georeferenced by a central point and

10.1029/2024WR039078

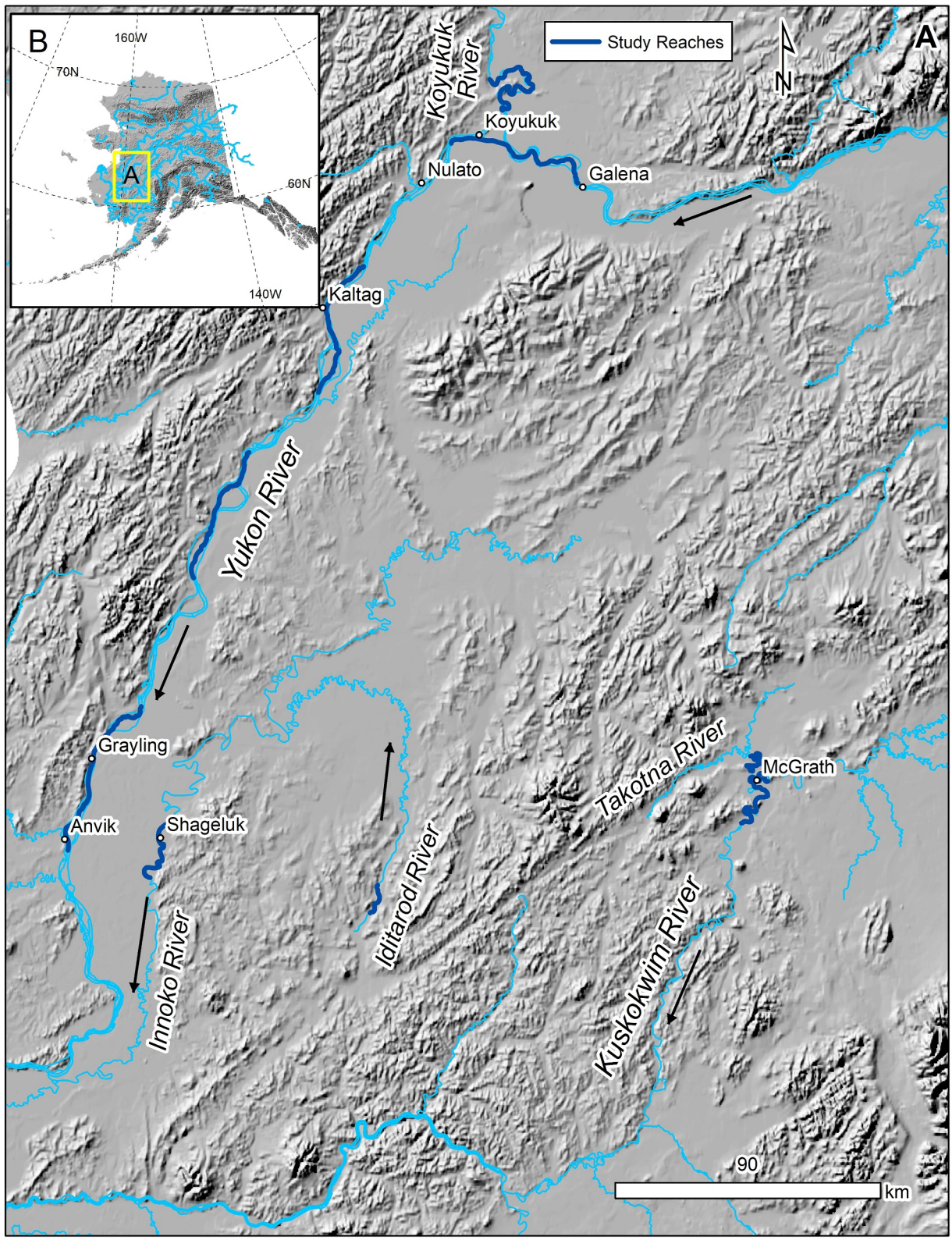

Figure 1. Study reach locations within the drainage system of the Yukon and Kuskokwim rivers and their tributaries (a) in western Alaska, USA (b) (black arrows indicate flow direction).

Table 1
Study Reach Locations and River Characteristics

River	Adjacent communities	Study reach length (km)	Channel width (m)	Slope (%)	Sinuosity	Form
Kuskokwim	McGrath	44.3	270	0.0135	2.4	Meandering
Takotna	McGrath, Takotna	21.9	90	0.0014	3.2	Meandering
Yukon	Galena, Koyukuk, Nulato	55.0	1,330	0.0073	1.2	Anastomosing
Koyukuk	Koyukuk	53.2	350	0.0075	1.8	Meandering
Yukon	Kaltag	52.7	1,910	0.0008	1.1	Anastomosing
Yukon	Eagle Island[a]	49.0	2,010	0.0061	1.1	Anastomosing
Yukon	Grayling, Anvik	59.5	1,390	0.0019	1.1	Anastomosing
Innoko	Shageluk	31.9	230	0.0063	1.4	Meandering
Iditarod	Iditarod City[b]	14.8	50	0.0270	1.7	Meandering

[a]Indicates that the name is of the nearest landmark. [b]Indicates that the community is abandoned and without year-round residents.

measured at the long axis, which was almost always in the direction of river flow (examples in Figures 2b, 2e, 2h and 2k). The same procedure was followed to identify OWZs during the early winter (late November) of the preceding years from 2017 to 2021 and late winter (March) from 2018 to 2023. This inventory of an additional five winters yielded 312 OWZs in early winter and 24 OWZs in late winter. A summary of satellite images used for all years and seasons is provided in Table S1 of Supporting Information S1. It is noted here that the timing and availability of imagery relative to the freeze-up sequence on each river was a distinct source of uncertainty particularly due to cloud cover. Interannual consistency in location of OWZ formation initially identified in the early winter of 2022 is reported as a ratio of winter seasons observed to total study winter seasons for both early and late winter periods. The analysis of interannual consistency in OWZ location was performed on the set of all OWZs in both early ($n = 359$) and late winter ($n = 29$), which ranged from a score 0.17 (i.e., an OWZ formed in only one of six study years) to 1.0 (i.e., OWZs formed at the same location in all six study years). Seasonal persistence for this study was defined as OWZs that were observed in both early and late winter. In only four cases (13%) did we observe an OWZ in late winter that was not visible in early winter at the same location. The size of OWZs are reported as the curvilinear length. For comparisons among study reaches, we report OWZ size as length per reach-averaged channel-width to standardize for river size and report OWZ density as the number per total study-reach length (Table 1).

2.3. Field Surveys

The subset of OWZ locations were visited between 11 and 23 March 2023. We were typically able to sample one to three OWZ locations per day among travel, other field studies, and community-outreach activities. As a standard safety procedure, our team of three always navigated to early freezing zones adjacent to OWZ locations (REFs) first and measured ice thickness to ensure conditions were safe in the area where ice had been growing the longest. Next, while two team members began sampling and data collection, one person drove a snowmachine with no sled to the OWZ-T site to check ice thickness while being spotted by the other team members. This was then repeated at the OWZ-H site before returning to the REF site to complete measurements. In practice, overflow (ponded water atop ice and often below the snowpack surface) was as much a concern as thin ice, but fortunately we found no ice thinner than 40 cm (>25 cm is considered safe for snowmachine travel) and most overflow we encountered did not limit our travel. Of the 23 sites originally selected for field data collection, we were able to completely sample 18. Two were only partly sampled due to open water still being present at OWZ-T and OWZ-H locations. At one OWZ location, the entire area still had open water and was unsafe to sample, and two were in locations where overflow made the approach too hazardous.

At each site category associated with an OWZ location (REF, OWZ-T, and OWZ-H), we drilled three holes spaced approximately 5-m apart through the ice column with 3-cm diameter Kovacs auger to measure ice thickness with snow depth recorded at the same three locations. An ice core was also collected at each site (three cores per OWZ location) using a 7.3-cm diameter Kovacs (Mark III) 1-m core-barrel driven with a rechargeable drill. Cores were photographed and subsampled for the presence of sediment and stratigraphic notes were made as described and reported in C. Arp et al. (2024), C. D. Arp et al. (2024). At the same three core-barrel auger holes,

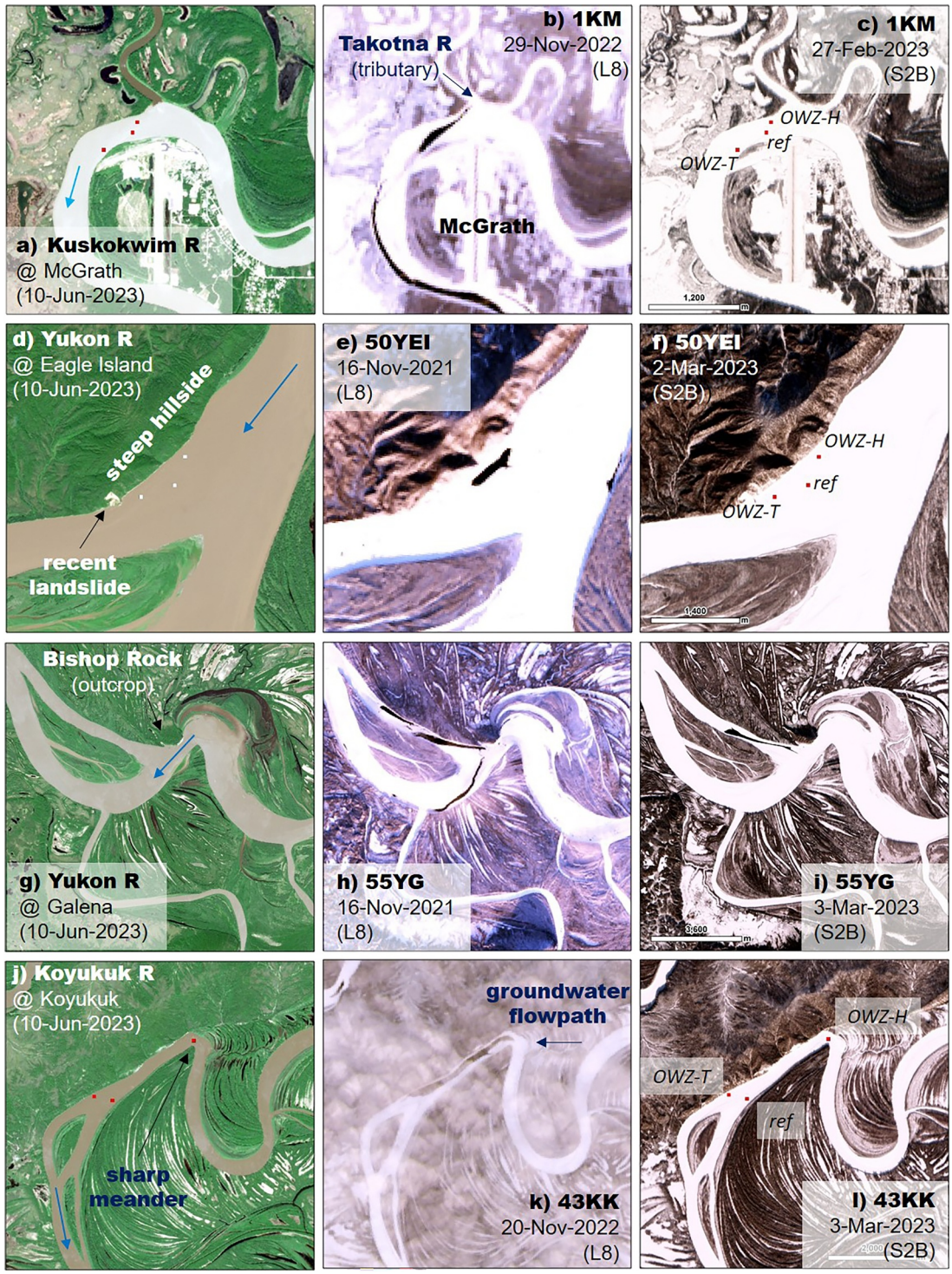

Figure 2. Examples of open-water zones locations in varying hydrogeomorphic settings paired by summer (a, d, g, j), early winter (b, e, h, k), and late winter (c, f, i, l). Summer images are all from Sentinel 2A, L8 is Landsat 8, and S2B is Sentinel 2B. Blue arrows indicate flow direction and sampling locations within sites are OWZ-H (upstream heads of OWZs), OWZ-T (downstream tails of OWZs), and ref (are reference locations adjacent to OWZ were ice cover was present at the time of early winter image acquisition).

we measured water depth and recorded velocity profiles for three 40-s intervals using an acoustic doppler current profiler (ADCP, RDI Teledyne StreamPro WaterMode 12). To detect any influence from groundwater upwelling, water temperature and specific conductance were measured at three depth intervals (below the ice surface, above

the river bed, and ~30 cm into the river bed sediment) using a profiling probe (Solinst 107 TLC) affixed to multiple 1.2-m section steel rods. The probe was held at each interval until temperature and specific conductance readings stabilized (typically 1–5 min at each interval). Our expectation was that any groundwater upwelling that could have an impact on surface ice formation would first be detectable in river-bed sediments by higher water temperature and specific conductance and then result in higher levels at the river bed and below the ice surface. Readings were repeated going both down and up through the water column to obtain a three-point profile at each sampling location. Unpersoned Aerial System (UAS) photos were collected at most sites when weather conditions allowed and surface snow and ice conditions were noted at each site.

2.4. Temporal and Spatial Analysis of Patterns and Processes

All inventoried OWZs among our nine study reaches and six winters were summarized according to size (length), standardized size (length per average channel width), extent (total length of OWZs per study-reach length), and density (number of OWZs per study-reach length). Comparisons of interannual variability to air temperature and discharge were made by summarizing all reaches together per winter to assess and understand general relationships. For air temperature, we used National Weather Service climate station records from Galena (USC00503212) and McGrath (USW00026510) together (averaged daily data) as the best representation of all study reaches (Figure 1). We calculated accumulated freezing degree days (AFDD) from the first day of average sub-zero temperature to the mean date of image acquisition (Table S1 in Supporting Information S1) for both early and late winter periods from 2017 to 2023 and compared these to OWZ extent and density by linear regression analysis. Because river discharge data is very limited by gauging stations that operate through the winter, we used mean monthly flow records from the Yukon River at Pilot Station (USGS 15565447, approximately 300 km downstream of Anvik) as the best consistent representation of regional river flow for our nine study reaches. Early winter (late November) OWZ extent and density were compared to averaged October and November discharge and late winter (late February to March) OWZ extent and density were compared to averaged December through March discharge also using linear regression analysis.

In order to understand spatial patterns of OWZ locations, we chose to classify the hydrogeomorphic setting as a way to organize these locations relative to landscape and fluvial form that were hypothesized to influence OWZ formation and persistence. Our three geomorphic (valley, channel, and bedform associated) and four hydrologic (bank erosion, tributary, hydraulic and groundwater associated) categories should be considered qualitative, yet they offer an important first-order organization of OWZ locations. This classification is described fully in the Supporting Information S1 (Text S1 in Supporting Information S1). Briefly and generally, in the geomorphic classification *valley-associated* refers to reaches contacting steep hillsides, *channel-associated* refers to reaches with high sinuosity or abrupt changes in width, and *bedform-associated* refers to reaches with notable bars, islands, or other shear zones. In the hydrologic classification, *tributary-associated* refers to reaches immediately downstream of tributary confluences, *groundwater-associated* refers to reaches with likely lateral subsurface flowpaths (i.e., below meander bends or abandoned side-channels), *bank erosion-associated* refers to reaches next to high cut-banks that were primarily observed during field visits, and *hydraulic-associated* refers to reaches subject to higher turbulence or shear zones observed in summer imagery with silty water. In addition to classifying these OWZs with the above taxonomy, we developed a set of hydrogeomorphic metrics to quantitatively compare these classes and potential controls on OWZ presence and extent. These metrics included local sinuosity (Dutton, 1999), channel-width dynamics, local channel and hillside slopes, and tributary impact with details provided in Supporting Information S1 (Text S1 in Supporting Information S1). Quantifying and comparing these metrics were important steps in testing whether our hydrogeomorphic classes were distinct and could result in a predictive model of OWZ size, interannual consistency, and persistence.

A general lack of explanatory success provided by the former hydrogeomorphic classification and quantification to understand OWZ size and interannual consistency suggested the role of other processes operating beyond the reach-scale. Our field observations and insights from the river-ice literature led us to more carefully examine the freeze-up process in available satellite imagery. Thus, we went back to the Planet Explorer (Planet Labs PBC, 2023) image archive to look more closely at the freeze-up sequence leading to early winter OWZs. In a high proportion of cases, we noticed that distinct freeze-up ice jams had formed upstream several weeks to a month before isolated open-leads (i.e., OWZs) were observed in late November imagery. Ice-jam formation was best indicated by the following sequence of observations in high-resolution images: (a) continuous open-water, (b) increasing concentrations of ice pans and expanding border ice, and (c) full channel bridging at a point with

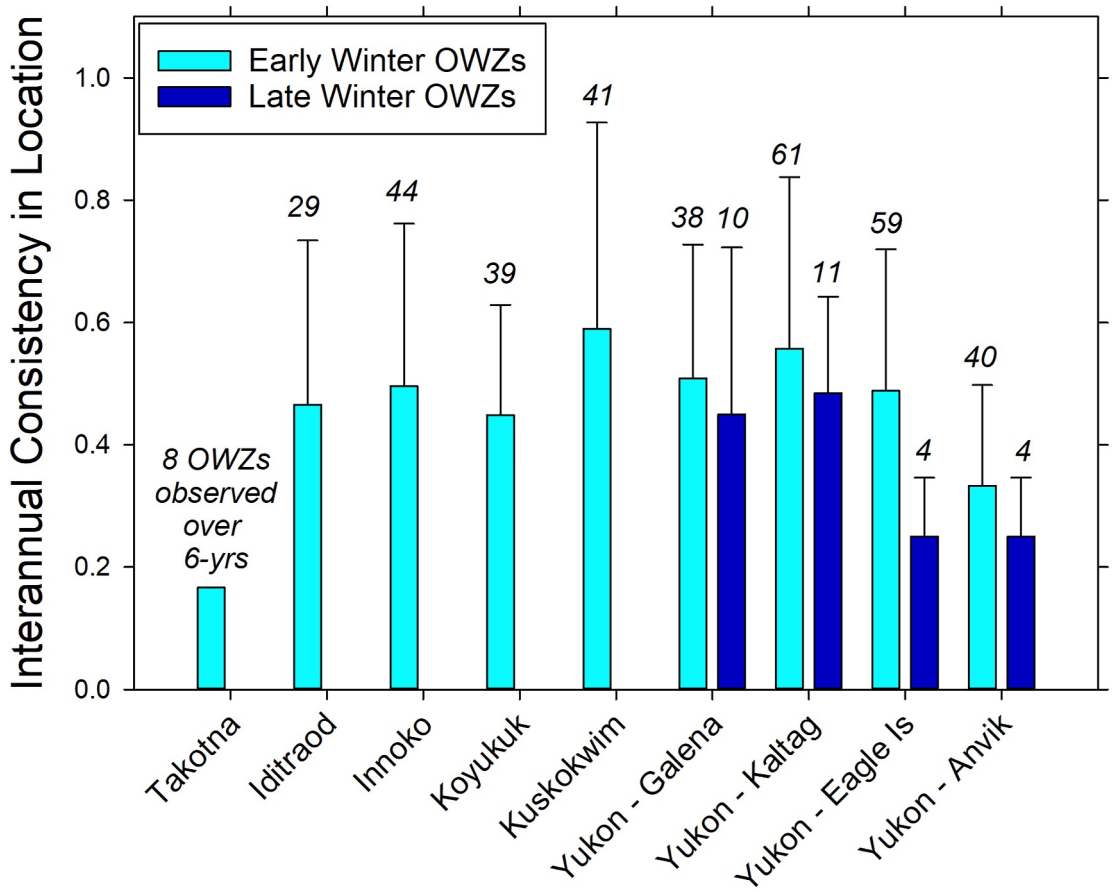

Figure 3. Interannual consistency of open-water zones (OWZs) by study river-reach (arrayed from smallest to largest) in the early winter (2017–2022) and late winter (2018–2023) based on identification with available satellite imagery (bars are standard errors, numbers above bars are the total number of OWZs per reach over all 6 years.

upstream lodgment of ice pans and downstream open water. Accordingly, we mapped all detectable freeze-up jams within our study reaches over the same six early winters and compared these to locations of OWZs. Quantitatively, we designated OWZs as associated with ice jams (i.e., OWZ—ice-jam complex) if they occurred downstream within 2-channel widths of an earlier freeze-up ice jam location. At several ice-jam locations with subsequent ideal cloud-free high-resolution optical imagery, we were able to quantify longitudinal OWZ closure rates as the distance of upstream ice accumulation between image dates. Lateral narrowing of OWZs due to border ice encroachment was generally not detectable even in high resolution (3-m) imagery, though this process likely functions importantly in OWZ closure as well.

3. Results

3.1. Size and Distribution of Open-Water Zones Among Study Reaches, Seasons, and Winters

An initial inventory of open-water zones (OWZs) existing within late November ice-cover in 2022 identified 48 locations with extents longer than 60-m down-river distance among eight of nine study reaches. Most OWZs were much larger with a median size of 530-m length. The number of OWZ inventoried in 2022 was similar to the 6-year average of 60 locations over nine study reaches and 380-km of river (Figure 3). Within four of these study reaches on the Yukon in 2022, our largest study river, we located 26 OWZs averaging 1,400-m in length and occupying 19% of the otherwise ice-covered channel by distance. The upper-most reach at Galena had six, often expansive OWZs averaging 3,200-m long, the middle two reaches at Kaltag and Eagle Island combined had 18 OWZs averaging 860-m long, and the lowest reach at Anvik had only two OWZs spanning 400 and 1,100 m of channel distance. Along the Kuskokwim, the other large mainstem river studied, we found six OWZs averaging 540-m length and occupying 7% of the otherwise ice-covered channel by distance. The other 16 OWZs identified

in 2022 were along tributaries of the Yukon River and were shorter, averaging 500-m in length. These 16 OWZs still occupied substantial portions of their respective river channels, 8% by distance on average. A higher density of OWZs was found along the Innoko River (2.8 per 10-km of river) compared to the Iditarod and Koyukuk rivers (1.3 per 10-km of river). The Takotna River, a tributary of the Kuskokwim, was an exception with no OWZs detected during this initial inventory period in November 2022. Along this 22-km long study reach, we only identified eight OWZs over the entire 6-year period, all in late November 2019. In the other eight study reaches, numbers of OWZs were generally more consistent among 6 years of inventory, 2017–2022.

Analysis of the entire 6-year OWZ inventory according to interannual consistency showed that 24% occurred in that location only once (consistency score of 0.17), while 8% occurred in the same location every year (consistency score of 1.0). Overall OWZ interannual consistency averaged 0.48 among all study reaches and ranging from 0.17 on the Takotna River to 0.59 on the Kuskokwim River (Figure 3). Late winter interannual consistency in OWZs averaged 0.41 among 29 locations identified over 6-years—all on study reaches of the Yukon River (Figure 3).

Of the 48 OWZ observed in early winter 2022, only five appeared to persist through to late winter (March) and these were all located on the Yukon River. The open-water state of these locations was confirmed during field visits in mid-March 2023 and were photographed for comparison with Sentinel-2B imagery (Figure 4). These seasonally persistent OWZs were generally larger, averaging 2,900-m in length in late November, compared to other smaller Yukon River OWZs that froze-over by late winter, which averaged 900-m in length in late November. All seasonally persistent OWZs shrank considerably from early to late winter, by 71% on average. We were not able to confirm whether ice-cover had closed progressively to the dimensions observed in March or if these had closed completely and then reopened at some time prior to field visits or when optical imagery became available again with increasing light conditions. Analysis of OWZ winter persistence over the other 5 years showed more variation with only one persisting into late winter in 2020 and 2022, six in 2021, seven in 2018, and nine in 2019. Of this set of 29 OWZs identified in late winter over 6 years, all but four were also observed at the same location in early winter.

Comparison of OWZ extent and density during the early winter period among all study years showed an average of 60 OWZs (1 per 6 river-km) occupied 12.2% of total channel length. Overall OWZ extent was lowest in 2022 (8.0%) and highest in 2018 (22.7%), while OWZ density was lowest in 2017 (31 or 1 per 12 river-km) and highest in 2020 (76 or 1 per 5 river-km). OWZ density was generally inversely related to OWZ extent ($r = -0.60$, $p = 0.21$) indicating that in years with fewer open-leads, these tended to be larger. For all OWZ inventoried, the average length was 1,780 m and the median length was 500 m with 23 (7%) exceeding 5,000 m in length——four of these were on the Kuskokwim River and the rest were on the Yukon River. Among the four tributary study-reaches, the average OWZ length was 590 m and the median length was 310 m with seven OWZs exceeding 2,000 m in length and all on the Koyukuk River, which is of similar size at the Kuskokwim River mainstem (Table 1).

To provide a general examination of how OWZ extent related to hydroclimatic conditions, we compared air temperature in early and late winter as accumulated freezing degree days (AFDD) and river discharge from the Yukon River at Pilot Station to the total extent of OWZs in each year of our inventory. Early winter OWZ-extent was distinctly higher in 2018, which also had the lowest AFFD and corresponding warmest air temperature (−3.6°C Oct–Nov average), while less variation was observed in OWZ extent in the other 5 years (8%–12%) despite a range in AFDD from −239°C days (−5.1°C Oct–Nov average) in 2017 to −513°C days (−10.7°C Oct–Nov average) in 2021 (Figure 5a). Thus a slightly positive relationship was seen with OWZ extent and AFFD ($r^2 = 0.32$, $p = 0.24$), but most of this pattern was driven by 2018. River discharge (Oct–Nov average) explained even less variation in OWZ extent despite a range from 6,222 cms in 2021 to 8,724 cms in 2022 (Figure 5b). Only 29 OWZ were detected in late winter (Feb–Mar) among all study years and these were all located on study reaches of the Yukon River with extents ranging from 0.1% in 2019 to 3.4% in 2018 of total channel length. Air temperature in the form of AFFD explained 53% ($p = 0.11$) of the variation in late winter OWZ extent (Figure 5c) where the winter of 2019–20 was coldest (−21.9°C Nov–Feb average) and 2017–2018 was warmest (−13.2°C Nov–Feb average).

Comparisons of late winter OWZ-extent to winter discharge showed no relationship despite a range from 1, 870 cms for the 2017–2018 winter to 2,481 cms for the 2022–2023 winter (Figure 5d). Multiple linear regression models using both air temperature and discharge did not provide additional explanation of variability in OWZ

Figure 4. Example of study sites with open-water leads that persisted into March 2023 documented with through field visits and unpersoned aerial system (UAS) photographs (a, c, e) and satellite (Sentinel-2B) imagery (b, d, f). Red arrows in panels (b, d, f) indicate approximate camera position and direction. Note that 16YA (a) had frozen over by time we made this field observation.

extent for either early or late winter periods. We also examined potential relationships between broad hydroclimatic metrics (temperature and discharge) and OWZ density and location consistency, but found no correlation.

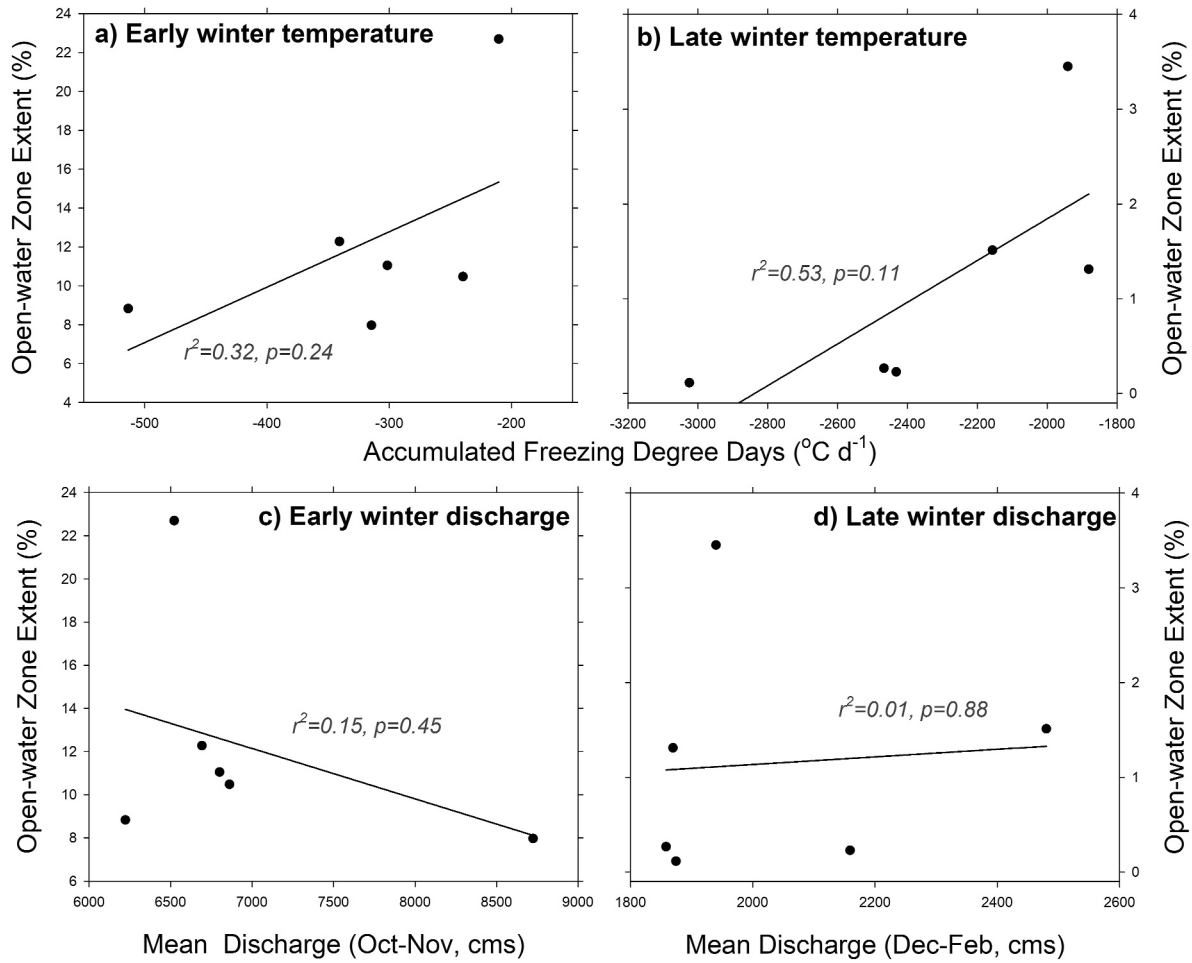

Figure 5. Comparison of inventoried open-water zone extents (summation of OWZ length per total study channel length) in detected in early winter (a, c) and late winter (b, d) imagery to air temperature (summarized as accumulated freezing degree days to the date of image acquisition from National Weather Service stations at Galena and McGrath) and river discharge (from USGS gage at Pilot Station on the Yukon River).

3.2. Field Characteristics of OWZ Locations

In addition to quantification of surface conditions, under-ice hydraulics, and physicochemical characterization of potential of groundwater influence, field visits to 18 OWZs in late winter 2023 provided essential validation of OWZ remote-sensing detection (Section 3.1), better informed hydrogeomorphic classification, and provided initial insights in the role of upstream ice-jams (Section 3.3). Channel islands and shadows in low-angle light conditions can appear similar to OWZs in even relatively high resolution optical imagery (i.e., Sentinel 2 at 10-m pixel size), yet every OWZ target we selected from late November 2022 imagery appeared to have been correctly identified based on field observations of either ice-cover atop flowing water or the presence of open-water in several cases (Figure 4). These conditions were verified at the specific points relative to each OWZ's upstream head (OWZ-H), downstream tail (OWZ-T), and adjacent river surface (REF) (see Figures 2c, 2f, 2i and 2l) where we collected field data in March 2023.

A large number of the earliest freezing sites (REF) adjacent to OWZs on the Yukon were within distinct jumble-ice fields or margins, whereas the many sites located within later freezing OWZ sites (OWZ-H and OWZ-T) were often impacted by liquid or refrozen overflow, which were generally uncommon in jumble-ice zones. A more limited set of sample locations on the Yukon, Iditarod, and Kuskokwim rivers were classified as black- or smooth-ice as indicated by the surface observations and ice cores. Snow depths measured in March at REF sites, which were identified as ice-covered in late November, were consistently deeper than adjacent OWZ-H and OWZ-T locations that were open in late November (Figure 6a). River ice thickness among all reaches and OWZ

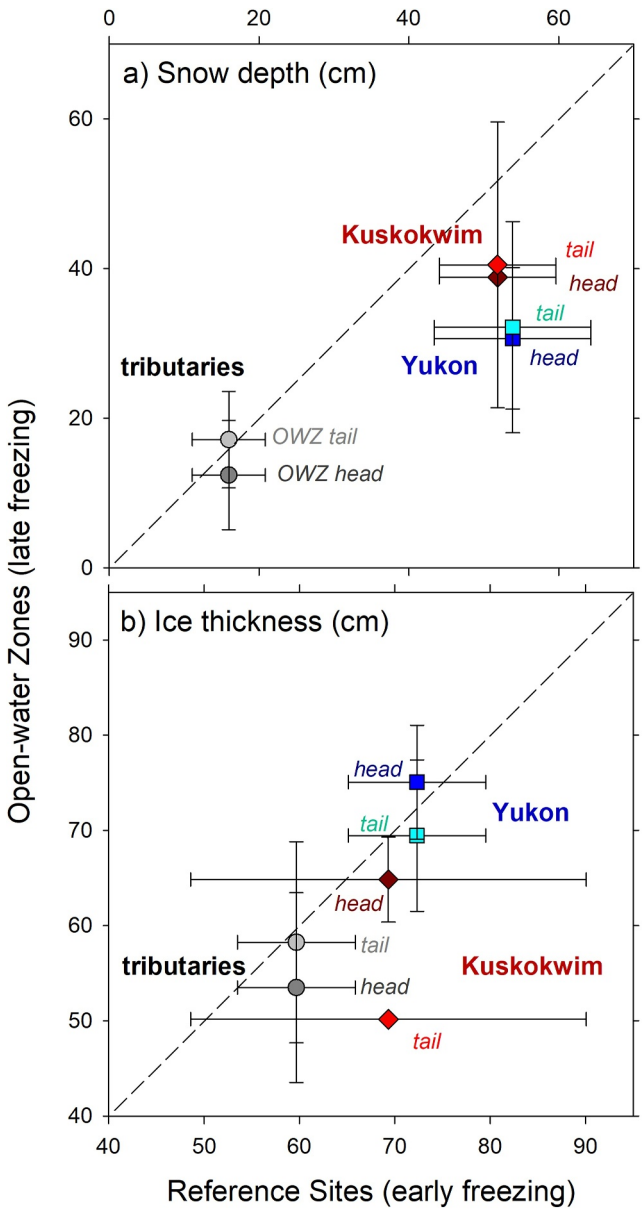

Figure 6. One-to-one comparisons of observed late winter (March) snow depth (a) and ice thickness (b) of open-water zones (later freezing, *y*-axis) to adjacent reference sites (earlier freezing, *x*-axis). Observations are presented as means and standard deviations grouped by OWZs on the Yukon River, Kuskokwim River, and tributaries of both rivers.

locations averaged 65 cm and ranged from an average of 51 cm on the Iditarod River to 72 cm on the Yukon River. Generally early freezing sites (REF) had ice thicknesses similar to adjacent late freezing sites (OWZ-H and OWZ-T) with a few notable exceptions where OWZ-location ice was distinctly thinner (Figure 6b).

Water temperature profiles (below the ice surface, at the river bed, and 30 cm into river bed sediments) collected at all sample locations averaged 0.4°C and were never warmer than 1.0°C. Specific conductivity averaged 850 uS/cm and ranged from 280 uS/cm on the Innoko River to 1,550 uS/cm on the Kuskokwim River with generally little variation within reaches. Most profiles showed slightly higher conductivity at the bed and into bed sediments, averaging 2% higher among all OWZ locations and above 10% higher at OWZ locations on the Iditarod River and one OWZ location on the Yukon River. Locations with higher increases in specific conductivity at the river bed tended to be shallower with fine gravel beds. Looking at the combined signatures of both temperature and specific conductivity at individual profiles showed only minor indications of groundwater or hyporheic mixing in bed sediments and no propagation of these waters to the under-ice surface where they could impact ice formation or growth.

All sites of field measurements had flowing water under ice with the exception of one location on the Innoko River that had frozen solid to the bed. River depths at sampling locations averaged 3.8 m and ranged from 1.3 m on the Iditarod River up to 4.8 m on the Takotna River, though several individual OWZ locations exceeded 7-m depth (the limits of our ADCP) and thus were not included in these reach-scale averages. Generally, rivers were deeper within OWZ sites compared to adjacent REF sampling sites that froze earlier (Figure 7a). Water-column velocities averaged 0.4 m/s and were lowest on average at Takotna and Iditarod river OWZ locations (0.2 and 0.3 m/s, respectively) and highest on average at Kuskokwim River OWZ locations (0.6 m/s). At the majority of late freezing OWZ sites, velocities were comparatively higher than adjacent early freezing REF sites (Figure 7b). Maximum water-column velocities did exceed 1 m/s in 12 sites, mainly on the Yukon and Kuskokwim rivers and mainly within OWZ heads or tails.

3.3. Analysis of Associations With and Causal-Factors of Open-Water Zones

All 48 OWZ locations initially identified in 2022 early winter imagery were placed into three geomorphic (valley-, channel-, and bedform-associated) and four hydrologic (tributary-, hydraulics-, groundwater-, and bank erosion-associated) classes, which were hypothesized to influence or cause open-water to persist in otherwise ice-covered rivers. The distribution of these classes was then compared among study reaches, according to OWZ size and interannual consistency (Figure 8), as well as hydrogeomorphic metrics intended to quantify and describe what these classes represented (Table S2, Figures S4 and S5 in Supporting Information S1). Most OWZ locations (78%) were geomorphically classified as either channel- or bedform-associated (see Figures S2 and S3 in Supporting Information S1 for examples). The remaining 11 OWZs were classified as valley-associated (see Figure S1 in Supporting Information S1 for examples) and tended to be large, seasonally persistent, and with higher interannually consistency (Figure 8a). Perhaps our best examples of a valley-associated OWZ was at Bishop Rock on the Yukon River below Galena where open-water persisted into late winter in nearly every study year (Figures 2i, 4e and 4f). Bedform-associated OWZs were smaller, averaging 595 m in length, compared to the other geomorphic classes, which averaged 1,215 m in length, and were also less interannually consistent (0.34) (Figure 8a). Hydrologic classification of OWZ settings explained little variation in size and interannual consistency (Figure 8b). Although geophysical quantification of OWZ settings also did little

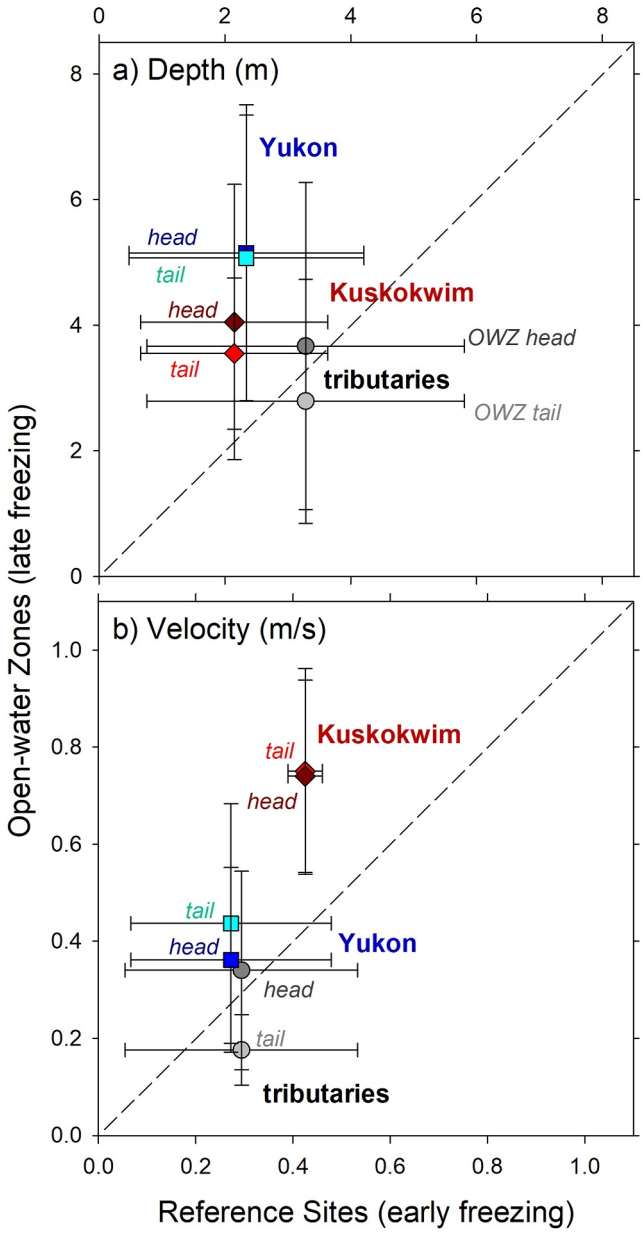

Figure 7. One-to-one comparisons of observed late winter (March) river depth (a) and water-column velocity (b) of open-water zones (later freezing, *y*-axis) to adjacent reference sites (earlier freezing, *x*-axis). Observations are presented as means and standard deviations grouped by OWZs on the Yukon River, Kuskokwim River, and tributaries of both rivers.

to distinctly separate these hydrologic classes, we note that channel slopes where OWZs formed were consistently steeper than reach-average slopes (Figure S5 in Supporting Information S1).

Over 6 years of winter freeze-up and down 380 km of river channel, we documented 359 OWZs that persisted into late November in otherwise contiguous ice cover. Over the same winters and river domains, we identified 175 ice jams during late October to early November. Well over half of these ice-jam locations (101) corresponded to the formation of one or more downstream OWZs (within two channel-widths or less) by late November (Figure 9). Freeze-up ice-jam density averaged one jam per 14 km over all study reaches and ranged from one jam per 20 km on the Kuskokwim River and up to one jam per 9 km on the Iditarod River. At ice jams co-occurring with later formation of OWZs downstream, densities among all reaches averaged one ice jam—OWZ complex per 20 km and ranged from one complex per 71 km on the Yukon River study-reach at Anvik (including 2 years with none observed), up to one complex per 10 km on the Innoko River. OWZs that appeared to be independent of upstream ice-jams were more abundant in all years, albeit to varying degrees, and also relatively smaller in size compared to OWZs associated with ice jams as a complex (Figure 10).

Closer inspection of early winter imagery showed that most freeze-up ice jams formed by early November, followed by upstream accumulation of ice (lodgment or juxtapositioned ice pans) advancing between ice-jam locations, typically leaving distinct OWZs in place by late November. On the Innoko River, two distinct locations associated with sharp meander-bends caused ice-jams in all study years, corresponding with at least one downstream OWZ at each location (Figure 11). Analysis of the position of the accumulation front to the next upstream ice jam showed a decreasing rate of OWZ closure over time; from 743 m/d over a 2-day period, to 560 m/d over the next 4 days, and a much slower rate of 72 m/d up to 12-Nov and leaving a 300-m OWZ (Figure 11d). Five other locations on the Innoko River developed freeze-up ice jams in some years, but not others, and three of these produced OWZs, while only one observed OWZ never was associated with an ice jam that we could see in available imagery. Another good example of ice jam—OWZ interactions came from the Kuskokwim River where a very consistent ice jam formed in all 6 years of observation at a sharp meander-bend intersected by the Takotna River confluence (Figure 2b), resulting in at least one OWZ persisting into early winter in all years. In the case of 2017 at this same point on the Kuskokwim, an open-lead persisted far downstream at least until 20-Nov. The occurrence of other OWZs on the reach of the Kuskokwim appeared dependent on the behavior of this primary freeze-up ice jam, where in some years multiple ice jam—OWZ complexes formed upstream and downstream and in other years only this primary complex formed below the Takotna River confluence (Figure 2b). On the Koyukuk River, a combination of cloud-free Planet, Sentinel, and Landsat imagery available in the late autumn and early winter of 2022, provided an excellent example of a dense, continuous run of pan ice on 26-Oct (Figure 12a), followed by multiple ice-jams in place 3-days later (Figure 12b), and then followed by three distinct OWZs remaining downstream of these same ice-jams by 20-Nov (Figure 12c). OWZ closure rates measured between 29-Oct and 20-Nov at these three locations averaged 38 m/d for this reach of the Koyukuk River, similar to the final and longer period of OWZ closure on the Innoko River of 72 m/d (Figure 11d).

Early winter ice-jams on reaches of the Yukon River were also observed, but their formation and form on this much larger and multi-channel anastomosing river were distinct from those in the smaller channels in this study. On the Yukon River, freeze-up ice jams were rarely observed to bridge the entire channel and often appeared

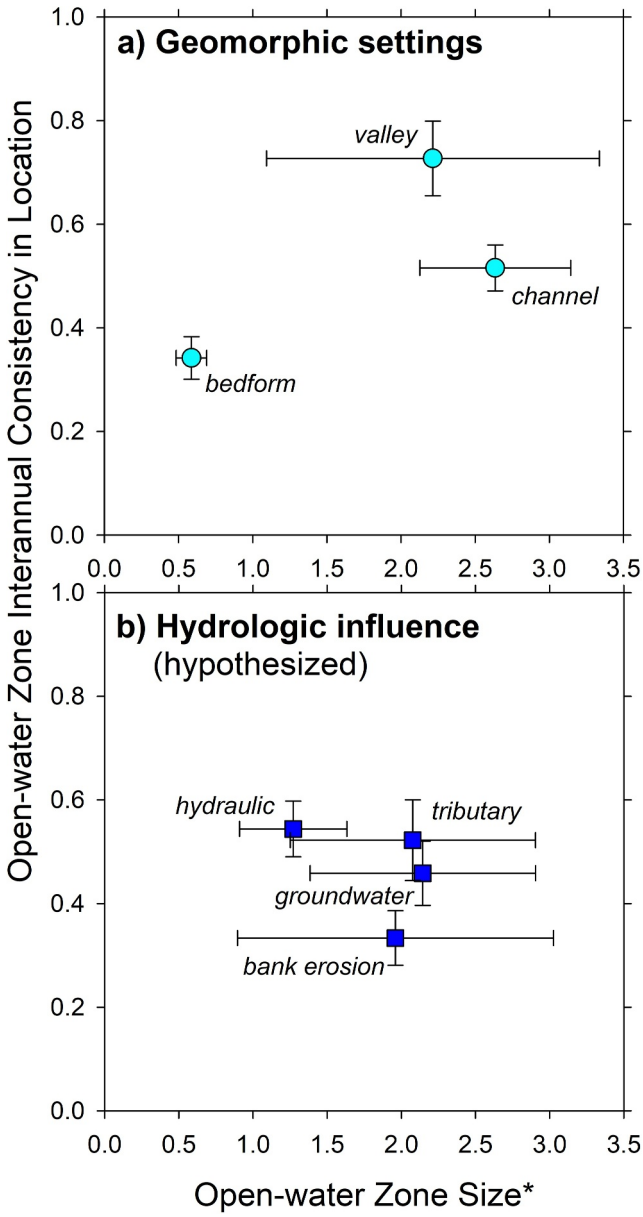

Figure 8. Comparison of 2022 early winter open-water zones by interannual consistency (i.e., recurrence frequency in the same location in 2017–2021) and open-water zone size* (OWZ length per reach-averaged width) and grouped by geomorphic setting (a) thought to influence late freezing status and hypothesized hydrologic influence (b) on late freezing status (bars are standard errors).

transient (i.e., ice-jam formation and release were observed in multiple cases when multi-temporal imagery was available). Thus on, The Yukon River, freeze-up ice jams were observed to produce downstream OWZs less frequently (Figure 10) and the exact location tended to vary more from year to year. An Exception to this pattern on the Yukon River was at Bishop Rock downstream of Galena (Figures 2g, 2h and 2i), at a location just below a sharp bend that is deep, narrow and turbulent, and notorious for causing impactful break-up ice jams. At this *valley-associated* location, an early winter OWZ developed in every year and remained open until late winter in most years downstream from where a freeze-up ice jam consistently formed within a tight temporal window between late October and early November in five out of 6 years.

4. Discussion

4.1. Ice-Jams and Open-Water Zones in Downstream River Continua

Current understanding of where and why open leads and polynyas (i.e., OWZs) develop and persist in ice-covered rivers is limited by a number of factors including challenges in observing these phenomena with remote sensing (Brown et al., 2018; Engram et al., 2024), identifying causal mechanisms through field observations and modeling (Jones et al., 2015), and establishing a link to broader-scale changes in northern rivers and their watersheds (Saros et al., 2022). We approached this question in part for our own travel safety concerns and more importantly for Alaska river travelers in general, as well as the need to advance our understanding of ice processes in northern rivers. Our study design attempted to balance spatial scales (9 river-reaches of varying size), temporal scales (six winter seasons), and a combination of remote sensing and field studies that could be reliably accomplished over these scales. Our idealized goal of explaining and predicting OWZs through a quantitative model is premature at this point, yet the results from this study led us to a new ice-jam hypothesis and a conceptual model (partially depicted in Figure 13) that we think advances mechanistic understanding and provides an improved basis for prediction.

We suggest that early winter OWZs in medium-to-large northern rivers primarily form downstream of ice jams during the freeze-up period for two main reasons. First, freeze-up ice jams disrupt downstream ice transport that otherwise would contribute to the development of full bank-to-bank ice cover (Figures 13a and 13b). This phenomenon was well observed in several study reaches through sequential image analysis (Figures 11 and 12), spatial co-occurrence of freeze-up ice jams with OWZs throughout our study reaches (Figures 9 and 10), and has strong basis from knowledge of the freeze-up process in many northern rivers (Das et al., 2015; Osterkamp & Gosink, 1983; Shen, 2010). The second reason is that the hydrogeomorphic settings that lead to initial freeze-up ice jams are locations generally associated with higher velocities and turbulence (Blackburn & She, 2019; Shen, 2010), which are very likely also present downstream of eventual jam-points (Figure 13a) and may become amplified after jams form due to channel constriction by ice (Figures 13b and 13c) (Das et al., 2015). We have not yet successfully quantified the channel hydraulics associated with ice-jam locations near or after the time of formation nor the downstream impacts once in place. Yet field data collected at OWZ locations later in the winter (Figure 7b), coupled with the fact that higher velocities will slow or prevent permanent ice-cover formation and growth (Lindenschmidt, 2020; Shen, 2010), support this likely feedback among jam formation, amplified velocities and turbulence, and slowed ice-cover growth (Figure 13).

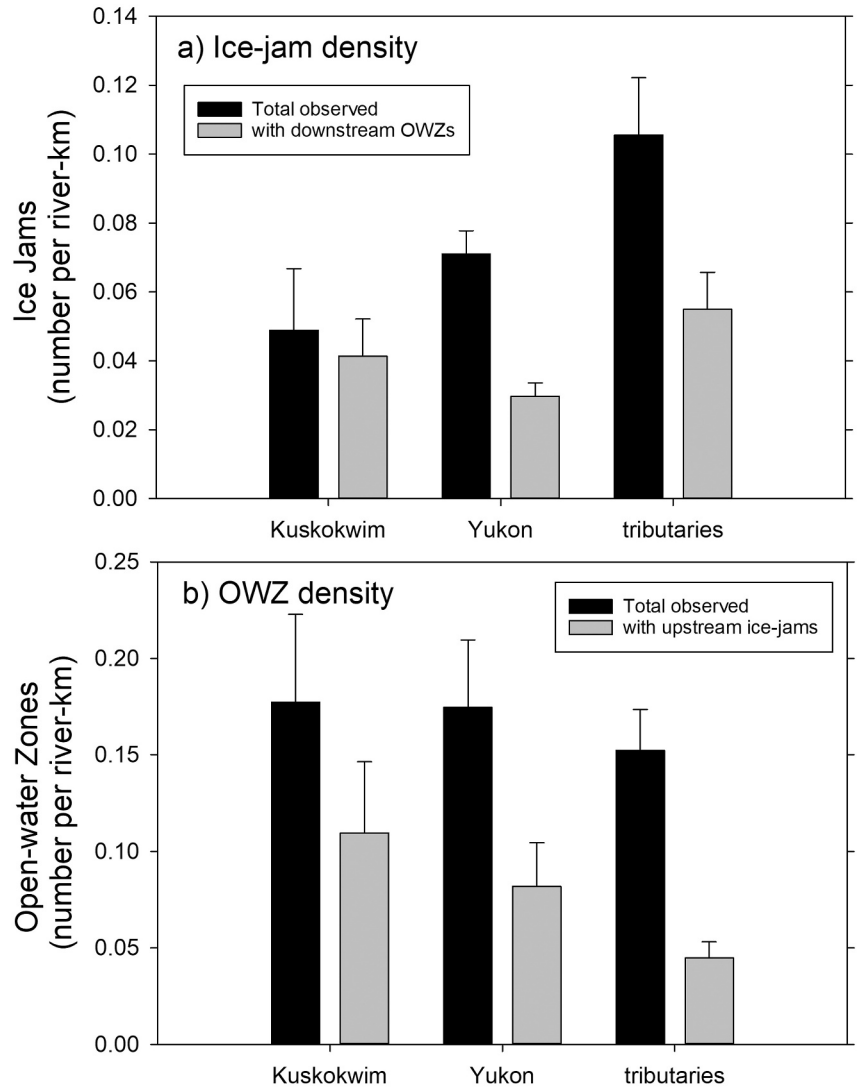

Figure 9. Ice-jam (a) and open-water zone (b) density per study channel distance averaged over all six study years (bars are standard errors).

Hydrogeomorphic classification and metrics, along with field data, provided insights into river characteristics allowing OWZ formation, persistence, and interannual consistency in location, yet these hypothesized explanatory factors only partially account for the continuous nature of rivers. Downstream ice transport in the form of frazil ice and ice pans interacts with border ice to develop full winter ice-covers in most medium-to-large northern rivers (Bergeron et al., 2011; Osterkamp & Gosink, 1983). Considering the location of ice jams during the early freeze-up period (currently late October to early November at our study rivers) relative to OWZs identified in late November provided a key link in our understanding of this process. The enhanced interannual consistency of OWZs classified as valley-associated (Figure 8a), as well as propensity of this class to persist into late winter at several reaches of the Yukon River, follows the general observation of ice-jam formation at or above channel-contacting outcrops that are often associated with steepening river slopes or slope breaks (Burrell et al., 2021; Das et al., 2015; Turcotte & Morse, 2013), and associated turbulence including eddies formed by colluvial inputs (Bergeron et al., 2011). Ice jams also form at sharp meander-bends and zones of channel narrowing (Das et al., 2015; Osterkamp & Gosink, 1983) unassociated with valley hillside confinement or rock outcrops (i.e., channel-associated class), as well as zones of channel widening and shallow bars (i.e., bedform-associated class) that can cause ice pans to ground and potentially cause full channel bridging in some years. Our observations of lower interannual consistency at OWZ locations classified as bedform-associated (Figure 8a) follow the

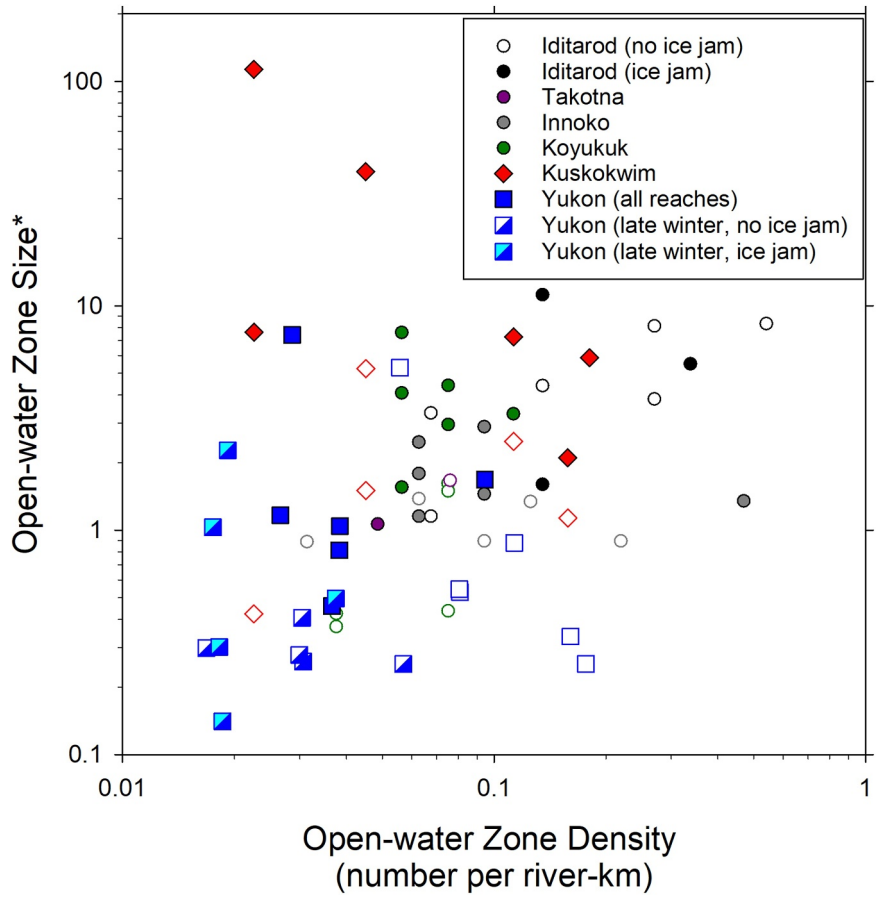

Figure 10. Summary of all observed open-water zones by relative size* (length per reach-averaged channel width) and density (number per river-km) averaged over all study years (2017–2023) and grouped as independent of ice jams (hollow symbols) and ice-jam associated (solid symbols).

expectation that freeze-up ice jams are more transient at these locations with varying river levels and bedform migration patterns. Reports of OWZs near shifting sandbars on the Yukon River (Herman-Mercer et al., 2011) likely fit with this category of bedform-associated OWZs in this study, which may relate to upstream freeze-up ice jams caused by ice-pan grounding that shift river currents and cause and sustain open leads. On large anastomosing channels like the Yukon River, ice jams in one channel can divert flows to another, making OWZ prediction more challenging.

Models of the sequence and downstream progression of freeze-up as proposed by Bergeron et al. (2011) advance our understanding of ice-cover evolution at river system scales. Formation of border ice along slow-water margins and production of frazil ice in more turbulent flow initiate with freezing air temperatures (Figure 13a). As temperatures continue to drop, runs of pan ice episodically increase in size and density, merging with border-ice constrictions, and eventually bridging (jamming or arresting) the full channel at multiple locations to form locally contiguous ice-covers that build upstream with continued pan-ice accumulation that decrease over time (Figures 11 and 12). Open-water zones below ice jams become important to continued frazil-ice production and subsequent downstream ice-pan formation (Barrette & Lindenschmidt, 2023; Osterkamp & Gosink, 1983), which then contribute to downstream ice-cover accumulation above the next jam point (Morales-Marin et al., 2019). Depending on temperature regimes and flow hydraulics, OWZs may eventually fill upstream and freeze-over completely with a consolidated ice cover (see contrasting scenarios in Figure 13d). Transport of frazil ice and ice pans under jam fronts likely plays an important role in the rate of OWZ longitudinal closure, while lateral narrowing due border ice growth is likely an important factor as well. The transport rate of upstream ice should increase with progressively cooling winter air temperature, but this is balanced with shrinking upstream frazil-ice production as OWZs close. Quantification of OWZ closure rates on the Innoko River show slowing accumulation

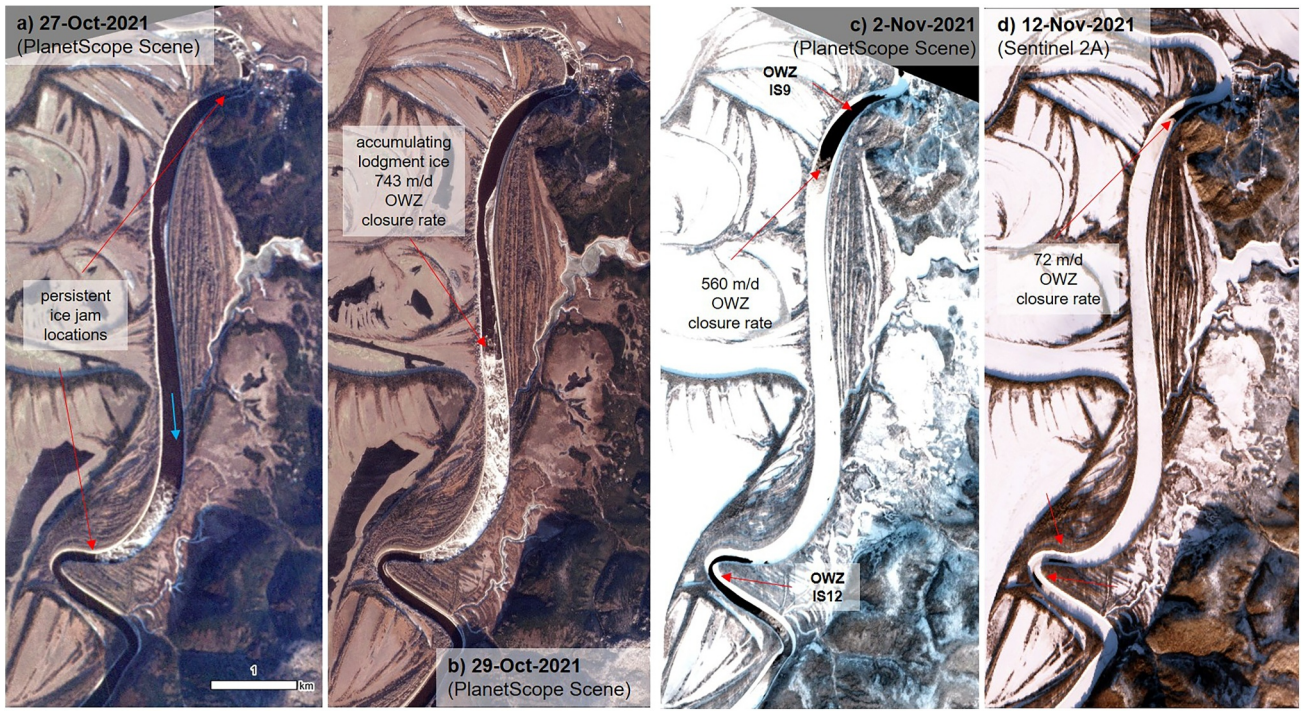

Figure 11. Time-series of high resolution satellite imagery during the freeze-up period of 2021 over a portion of the Innoko River study reach showing locations of ice-jam formation (a), subsequent upstream ice accumulation (b), and resulting of open-water zones (c, d). Open-water zone closure rates between each image are presented in panels (b, c, and d). Blue arrow indicates flow direction.

from the time of initial ice-jam formation, suggesting the importance of reduced upstream ice transport (Figure 11) with similar rates observed on the Koyukuk River (Figure 12). Continuing to improve our understanding of this freeze-up sequence and how it varies among climate settings and river sizes and forms will advance our ability to predict where and when OWZs form and persist. Taking a sequential view of river freeze-up in the context of climate change will also advance northern river science beyond simple freeze-up and break-up dates (Barrette & Lindenschmidt, 2023; Brown et al., 2018).

4.2. Winter Open-Water Zones in a Changing Climate

Much recent interest exists as to how river ice is responding to climate change in Alaska and other high latitude regions (e.g., Barrette & Lindenschmidt, 2023; Brown et al., 2023; Burrell et al., 2021). Warmer winter air temperature is a first order cause of later and prolonged freeze-up and higher river flows are considered to cause similar delays in ice-cover formation (Beltaos & Prowse, 2009). Specifically regarding observations of OWZs, traditional and local knowledge suggests these river hazards are increasing in abundance and persistence in recent decades (Brown et al., 2018; Herman-Mercer et al., 2011; Miller, 2023; Wilson et al., 2015) and long-term change detection analysis supports these observations in the context of changing air temperature and river discharge (Brown et al., 2023). The relatively short time-period of our study (6 years) precludes rigorous analysis of the role of temperature and discharge in the abundance, size, interannual consistency, and winter-long persistence of OWZs. Simple comparison of year-to-year variability relative to regional air temperature and discharge provided limited evidence that warmer wetter early winters cause more or more extensive OWZs to initially form (Figures 5a and 5b), though warmer late winters likely relate to OWZ persistence on the Yukon River (Figure 5c) and at least conceptually higher winter baseflows should cause OWZ persistence as well (Beltaos & Prowse, 2009, Figure 13d). With that said, the distinctly warmer early winter of 2018 and corresponding more extensive OWZs (Figure 5a) were particularly notable according to long-time observers along the Yukon River. With respect to the role of winter discharge in OWZ persistence into late winter (Figure 13d), future work examining finer-scale variability in under-ice discharge may eventually prove consequential in understanding this process. Yet quantifying under-ice discharge, particularly on large rivers, is currently limited to labor-intensive

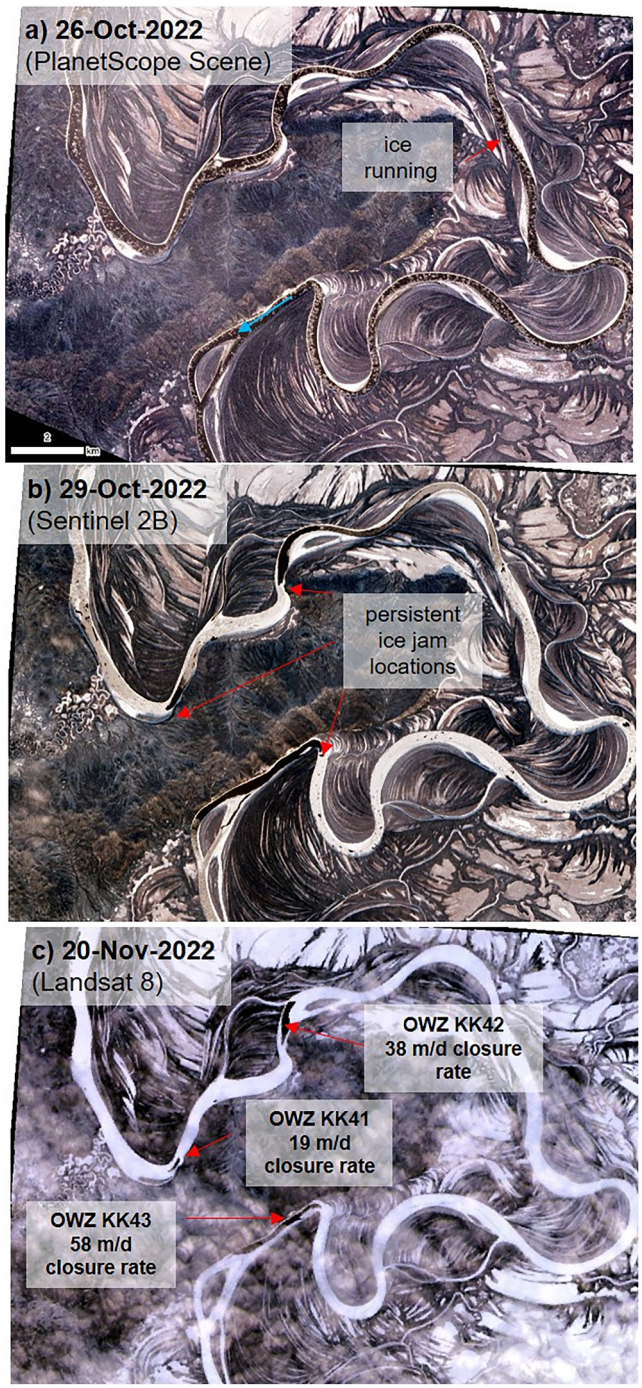

Figure 12. Time-series of high to medium resolution satellite imagery during the freeze-up period of 2022 over a portion of the Koyukuk River study reach showing a continuous ice-pan run (a), development of multiple ice-jams (b), and corresponding persistence of open-water zones below these ice-jams (c). Open-water zone closure rates between images are presented in panel (c).

and often inaccurate point measurements with interpolation between points, making understanding of winter hydrology in large northern rivers an ongoing challenge.

Observations of higher winter discharge in northern rivers, including the Yukon, are often explained by warmer air temperatures and a complex interplay among permafrost degradation, enhanced groundwater storage, and higher levels of baseflow (Blaskey et al., 2023; Walvoord & Kurylyk, 2016; Walvoord & Striegl, 2007) and have followed as a suggested driver of OWZ behavior (Jones et al., 2015; Saros et al., 2022). Whether permafrost degradation is linked to higher baseflow in northern rivers, as opposed to higher contributions from late season rainfall (C. D. Arp et al., 2020) or glacial meltwater (Liljedahl et al., 2017), may eventually be resolved by scientists studying major northern river basins. In the case of OWZs in this and other studies in Alaska (e.g., Jones et al., 2015; Wirth et al., 2012), little evidence has been found confirming the role of groundwater upwelling in OWZ formation and persistence. Our field measurements of water temperature and specific conductance gradients from the river-bed to ice-surface in late winter never indicated distinct upwelling zones associated with OWZ locations. Data collection from a more limited set of OWZs on the Tanana River in interior Alaska detected upwelling zones in backwater sloughs, yet model sensitivity analysis from this same study suggested that water velocity was the more important factor in slowing ice growth (Jones et al., 2015). We also compared OWZs classified as groundwater-associated based on position relative to expected upwelling flowpaths (see Figure 2k for example), yet these locations were typically less seasonally persistent or interannually consistent than OWZ locations classified by river hydraulics and turbulence (Figure 8b). Admittedly the timing and scale of our field measurements collected in late winter, along with assumptions of our classification, do not necessary provide clear evidence as to the role of groundwater in forming and maintaining OWZs. Principles of heat transfer and ice growth suggest that groundwater upwelling should prevent or slow ice growth in settings of low specific discharge relative to warm groundwater influx (Shen, 2010), yet even in the case of backwater sloughs, this impact has been challenging to demonstrate (Jones et al., 2015). We suggest that in larger river channels where we studied OWZs, the flux and temperature of groundwater upwelling would need to be extreme (e.g., geothermal springs) to both detect and have an impact on ice formation. OWZs on side-channels and sloughs of these same rivers are often observed (Clawson et al., 2022; Jones et al., 2015) and we suspect that groundwater plays a role in their formation and persistence in many cases. What is likely more critical in forming OWZ in side-channels of larger rivers is small channel width relative to large drops in stage associated with declining discharge through the winter, which cause floating ice to crack and separate, allowing any shallow channel flow and groundwater contributions to help maintain OWZs. We have observed such conditions commonly when following side-channels shortcuts on the Tanana River, often resulting in delays or backtracking to the main channel.

4.3. Predicting Open-Water Zones for Hazard Assessment

From the perspective of a winter river traveler, the most dangerous places to traverse are recently frozen OWZs surrounded by otherwise thick and stable ice-cover in unexpected places. Our tracking of 359 early winter OWZs across 380 km of nine river-reaches over 6 years found that the vast majority froze-over later in the winter and only occurred in the same location half of the time. OWZs that occur in the same location every year and that remain open all winter are typically less hazardous

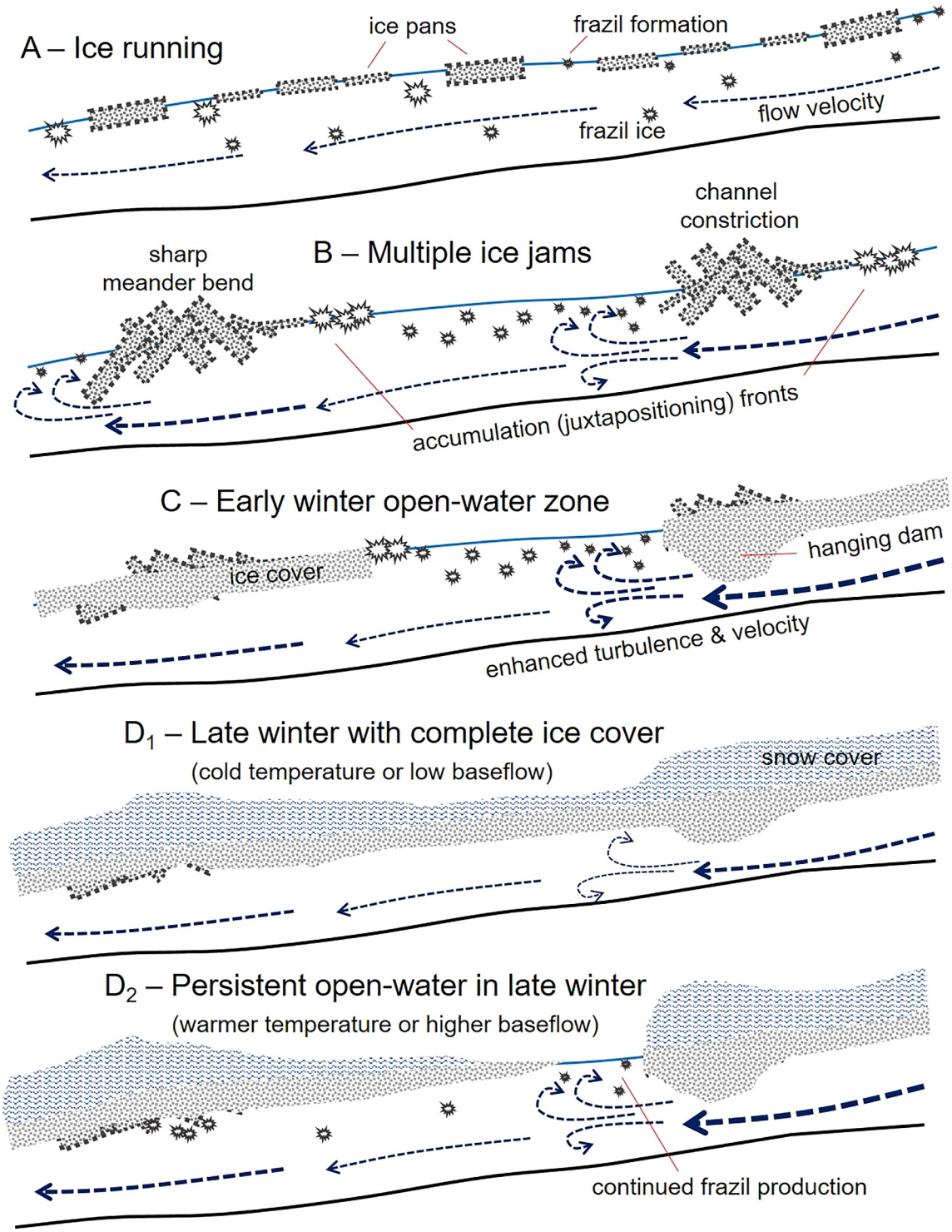

Figure 13. Conceptual diagram of the reach-scale river freeze-up processes from frazil-ice production and ice-pan transport (a), to ice-jam formation (b) and corresponding impacts on channel hydraulics (c) resulting in early winter open-water zones. Depending on following winter hydroclimatic scenarios open-water zones forming downstream of ice jams may freeze-over completed (D_1) or persist into late winter (D_2).

to experienced river travelers, though serious accidents happen almost every year in Alaska on frozen rivers due to travel in low visibility conditions (Fleisher et al., 2013). On the lower Kuskokwim River for example, community *Search and Rescue* volunteers regularly mark OWZs with cut willows to alert winter travelers among multiple

river-side villages to these hazards. On-the-ice observations and aerial reconnaissance flights, along with traditional and local knowledge, are essential for identifying and marking these hazards. Production of ice fog during very cold periods (e.g., >−30°C) is highly indicative of OWZs and also can generate an additional hazard for aviation into and out of river-side communities. For example, this aviation hazard was indicated by community members in Rampart, AK on the Yukon River in 2024. High-resolution optical satellite imagery, such as what we relied on in this study, is becoming increasingly available for detecting OWZ hazards in early winter, yet become very limited through December and January due to low light conditions. Use of synthetic aperture radar (SAR) satellite imagery (e.g., Sentinel-1) to detect OWZs is being actively developed (Engram et al., 2024; Wirth et al., 2012) and user-friendly web-based platforms to classify river ice conditions in near real-time are progressing to the point of practically aiding river-ice hazard mitigation (Abdelkader et al., 2024). The integration of radar and optical remote sensing with community member and citizen scientist observations, such as those documented through the *Fresh Eyes on Ice* program by citizen scientists across Alaska, is advancing hazard assessment on Alaskan rivers (e.g., Brown et al., 2023; Engram et al., 2024) and has the potential to create important positive feedbacks to the benefit of both remote sensing science and public education and safety (Clement et al., 2023).

Findings from this study suggest that freeze-up ice jams and associated hydraulics cause the formation of most OWZs on western Alaskan rivers and it follows that better understanding the mechanisms of freeze-up ice jams should provide the basis for predicting OWZ location and perhaps seasonal persistence. The vast majority of river ice-jam research has focused on the spring season when dynamic, mechanical break-up events can cause backwater flooding and ice-jam release waves (javes) (Beltaos & Prowse, 2009; Burrell et al., 2021; Lindenschmidt, 2020). While antecedent and weather conditions causing dynamic break-ups are relatively well understood, predicting where or when break-up ice jams will occur remains quite challenging (Beltaos & Prowse, 2009; Lindenschmidt, 2020). Very generally, observations suggest that break-up ice jams often recur at key locations with constricted channels or sharp meanders, similar to our observations of freeze-up ice jams. Regarding ice jamming during the freeze-up period, it is generally understood that rivers first need to transport frazil-ice pans, perhaps with increasing size and density, but very few details are known about when and where freeze-up ice jams occur (Burrell et al., 2021) and thus where and when OWZs will form downstream.

We suspect that many of the insights into the relationship between freeze-up ice jams and OWZ formation, consistency, and persistence we have gleaned from this study of western Alaskan rivers are already understood by many people who live by and travel on northern rivers. Similarly, we also suspect that many experienced river-ice scientists understand this relationship as well, but studying and communicating the processes driving OWZ behavior has taken lower priority compared to other river ice problems (e.g., break-up ice jams and flooding). Our hope is that this study, along with concurrent research on river-ice conditions and processes (e.g., Brown et al., 2023; Engram et al., 2024), will advance prediction of hazards at time- and space-scales applicable to rural community public safety. Fostering communication and feedback between ice scientists and rural river communities through schools (Clement et al., 2023), local *Search and Rescue* groups (Engram et al., 2024), and seasoned winter travelers (Schneider et al., 2015) is an important pro-active opportunity to improve hazard awareness and adaptation to ongoing climate change.

5. Conclusions

Freeze-up on northern rivers has been a challenging process to observe, understand, and predict particularly with respect to hazardous open-water zones (OWZs). Remote sensing detection and analysis of 359 OWZs along nine river reaches in western Alaska totaling 380 km indicate relative consistency in location from year-to-year with only a few regularly persisting through the entire winter. Field measurements at a subset of these OWZs show their channel locations are generally deeper with higher water velocities compared to adjacent earlier freezing locations and with no indications of groundwater upwelling. More consistent OWZs where associated with confined valleys, sharp meander-bends, and channel constrictions, which relate to observations of upstream ice-jams that formed during the earlier stages of freeze-up. Our hypothesis is that ice jams disrupt downstream ice transport and cause additional downstream turbulence, slowing ice accumulation and closure in the upstream direction, and thus lead to open-water persistence even during deep cold periods (<−40°C). Elucidating this ice-jam mechanism advances understanding of northern river freeze-up, yet requires more focused research to quantitatively document this complex interaction and explore alternative mechanisms causing OWZ formation. Perhaps of more general and immediate concern is understanding how and predicting to what extent climate

change in the form of warmer winters and increasing river discharge impact the formation of contiguous river ice-cover and the human and ecosystem services it provides.

Data Availability Statement

The primary field and remote sensing data set supporting this research is archived with the Arctic Data Center at (C. Arp et al., 2024) (https://doi.org/10.18739/A2086372J).

Acknowledgments
Financial support for this research was provided by the National Science Foundation (#1836523) and the National Aeronautical and Atmospheric Association (##80NSSC21K858) with logistical support provided by Polar Field Services, Inc. Two anonymous reviewers provided helpful and constructive comments on an earlier draft of this manuscript. Special thanks go to the communities, schools, students, and teachers of McGrath, Sleetmute, Shageluk, and Galena. In particular, we thank teacher-principals Matthew Shelborne, Angela Hayden, and Joyanne Hamilton for their hospitality, support, and insights during our field studies.

References

Abdelkader, M., Bravo, J., Temimi, M., Brown, D. R. N., Spellman, K. V., Arp, C. D., et al. (2024). A Google Earth Engine platform to integrate multi-satellite and citizen science data for the monitoring of river ice dynamics. *Remote Sensing*, *16*(8), 1368. https://doi.org/10.3390/rs16081368

Arp, C., Bondurant, A., & Clement, S. (2024). Winter open-water zone remote sensing (2017–2023) and field (2023) data from the Yukon and Kuskokwim rivers and their tributaries in western Alaska [Dataset]. *Arctic Data Center*. https://doi.org/10.18739/A2086372J

Arp, C. D., Bondurant, A. C., Clement, S., Eidam, E., Langhorst, T., Pavelsky, T. M., et al. (2024). Observation of high sediment concentrations entrained in jumble river ice. *River Research and Applications*, *40*(8), 1560–1570. https://doi.org/10.1002/rra.4309

Arp, C. D., Whitman, M. S., Kemnitz, R., & Stuefer, S. L. (2020). Evidence of hydrological intensification and regime change from Northern Alaskan watershed runoff. *Geophysical Research Letters*, *47*(17), e2020GL089186. https://doi.org/10.1029/2020gl089186

Barrette, P. D., & Lindenschmidt, K.-E. (2023). Frazil ice events: Assessing what to expect in the future. *Hydrology Research*, *54*(6), 770–781. https://doi.org/10.2166/nh.2023.008

Beltaos, S. (2013). River ice formation. In *Committee on river ice processes and the environment, Canadian geophysical union hydrology section*.

Beltaos, S., & Prowse, T. (2009). River-ice hydrology in a shrinking cryosphere. *Hydrological Processes*, *23*(1), 122–144. https://doi.org/10.1002/hyp.7165

Bennett, K. E., Schwenk, J., Bachand, C., Gasarch, E., Stachelek, J., Bolton, W. R., & Rowland, J. C. (2023). Recent streamflow trends across permafrost basins of North America. *Front. Water*, *5*, 1099660. https://doi.org/10.3389/frwa.2023.1099660

Bergeron, N. E., Buffin-Bélanger, T., & Dubé, J. (2011). Conceptual model of river ice types and dynamics along sedimentary links. *River Research and Applications*, *27*(9), 1159–1167. https://doi.org/10.1002/rra.1479

Blackburn, J., & She, Y. (2019). A comprehensive public-domain river ice process model and its application to a complex natural river. *Cold Regions Science and Technology*, *163*, 44–58. https://doi.org/10.1016/j.coldregions.2019.04.010

Blaskey, D., Koch, J. C., Gooseff, M. N., Newman, A. J., Cheng, Y., O'Donnell, J. A., & Musselman, K. N. (2023). Increasing Alaskan river discharge during the cold season is driven by recent warming. *Environmental Research Letters*, *18*(2), 024042. https://doi.org/10.1088/1748-9326/acb661

Brown, D. R. N., Arp, C. D., Brinkman, T. J., Cellarius, B. A., Engram, M., Miller, M. E., & Spellman, K. V. (2023). Long-term change and geospatial patterns of river ice cover and navigability in Southcentral Alaska detected with remote sensing. *Arctic Antarctic and Alpine Research*, *55*(1), 2241279. https://doi.org/10.1080/15230430.2023.2241279

Brown, D. R. N., Brinkman, T. J., Verbyla, D. L., Brown, C. L., Cold, H. S., & Hollingsworth, T. N. (2018). Changing River ice seasonality and impacts on interior Alaskan communities. *Weather, Climate, and Society*, *10*(4), 625–640. https://doi.org/10.1175/WCAS-D-17-0101.1

Burrell, B. C., Beltaos, S., & Turcotte, B. (2021). Effects of climate change on river-ice processes and ice jams. *International Journal of River Basin Management*, 1–21.

Clawson, C. M., Falke, J. A., Bailey, L. L., Rose, J., Prakash, A., & Martin, A. E. (2022). High-resolution remote sensing and multistate occupancy estimation identify drivers of spawning site selection in fall chum salmon (Oncorhynchus Keta) across a sub-Arctic riverscape. *Canadian Journal of Fisheries and Aquatic Sciences*, *79*(3), 380–394. https://doi.org/10.1139/cjfas-2021-0013

Clement, S., Spellman, K., Oxtoby, L., Kealy, K., Bodony, K., Sparrow, E., & Arp, C. (2023). Redistributing power in community and citizen science: Effects on youth science self-efficacy and interest. *Sustainability*, *15*(11), 8876. https://doi.org/10.3390/su15118876

Das, A., Sagin, J., Sanden, J. V. d., Evans, E., McKay, H., & Lindenschmidt, K.-E. (2015). Monitoring the freeze-up and ice cover progression of the Slave River. *Canadian Journal of Civil Engineering*, *42*(9), 609–621.

Dutton, G. (1999). Scale, sinuosity, and point selection in digital line generalization. *Cartography and Geographic Information Science*, *26*(1), 33–54. https://doi.org/10.1559/152304099782424929

Engram, M., Meyer, F. J., Brown, D. R. N., Clement, S., Bondurant, A. C., Spellman, K. V., et al. (2024). Detecting early winter open-water zones on Alaska rivers using dual-polarized C-band Sentinel-1 Synthetic Aperture Radar (SAR). *Remote Sensing of Environment*, *305*, 114096. https://doi.org/10.1016/j.rse.2024.114096

Fleischer, N. L., Melstrom, P., Yard, E., Brubaker, M., & Thomas, T. (2013). The epidemiology of falling-through-the-ice in Alaska, 1990–2010. *Journal of Public Health*, *36*(2), 235–242. https://doi.org/10.1093/pubmed/fdt081

Herman-Mercer, N., Schuster, P. F., & Maracle, K. B. (2011). Indigenous observations of climate change in the lower Yukon River basin, Alaska. *Human Organization*, *70*(3), 244–252. https://doi.org/10.17730/humo.70.3.v88841235897071m

International Association for Hydraulic Research Association. (1980). *Multilingual ice terminology Addendum I*. Published by the Research Centre for Water Resources Budapest. Retrieved from https://rivergages.mvr.usace.army.mil/WaterControl/Districts/MVP/Reports/ice/iahr_ice_terminology.html

Jones, C., Kielland, K., & Hinzman, L. (2015). Modeling groundwater upwelling as a control on river ice thickness. *Hydrology Research*, *46*(4), 566–577. https://doi.org/10.2166/nh.2015.026

Liljedahl, A. K., Gädeke, A., O'Neel, S., Gatesman, T. A., & Douglas, T. A. (2017). Glacierized headwater streams as aquifer recharge corridors, subarctic Alaska. *Geophysical Research Letters*, *44*(13), 6876–6885. https://doi.org/10.1002/2017gl073834

Lindenschmidt, K. E. (2020). *River ice processes and ice flood forecasting*. Springer International Publishing.

Magnuson, J. J., Robertson, D. M., Benson, B. J., Wynne, R. H., Livingstone, D. M., Arai, T., et al. (2000). Historical trends in lake and river ice cover in the Northern Hemisphere. *Science*, *289*(5485), 1743–1747. https://doi.org/10.1126/science.289.5485.1743

Miller, O. (2023). Traditional knowledge of changes in winter conditions in Alaska's Copper River Basin. Alaska Park. *Science*, *22*(1), 90–101.

Morales-Marín, L. A., Sanyal, P. R., Kadowaki, H., Li, Z., Rokaya, P., & Lindenschmidt, K. E. (2019). A hydrological and water temperature modelling framework to simulate the timing of river freeze-up and ice-cover breakup in large-scale catchments. *Environmental Modelling & Software*, *114*, 49–63. https://doi.org/10.1016/j.envsoft.2019.01.009

Osterkamp, T. E., & Gosink, J. P. (1983). Frazil ice formation and ice cover development in interior Alaska streams. *Cold Regions Science and Technology*, *8*(1), 43–56. https://doi.org/10.1016/0165-232x(83)90016-2

Planet Labs PBC. (2023). Planetscope. [online]. https://developers.planet.com/docs/data/planetscope/

Prowse, T., Alfredsen, K., Beltaos, S., Bonsal, B., Duguay, C., Korhola, A., et al. (2011). Past and future changes in Arctic Lake and River ice. *Ambio*, *40*(S1), 53–62. https://doi.org/10.1007/s13280-011-0216-7

Rice, S., & Church, M. (1998). Grain size along two gravel-bed rivers: Statistical variation, spatial pattern and sedimentary links. *Earth Surface Processes and Landforms*, *23*(4), 345–363. https://doi.org/10.1002/(sici)1096-9837(199804)23:4<345::aid-esp850>3.0.co;2-b

Saros, J. E., Arp, C. D., Bouchard, F., Comte, J., Couture, R. M., Dean, J. F., et al. (2022). Sentinel responses of Arctic freshwater systems to climate: Linkages, evidence, and a roadmap for future research. *Arctic Science*, *9*(2), 356–392. https://doi.org/10.1139/as-2022-0021

Schneider, W., Brewster, K., & Kielland, K. (2015). Team building on dangerous ice: A study in collaborative learning. *Arctic*, *68*(3), 399–404. https://doi.org/10.14430/arctic4516

Shen, H. T. (2010). Mathematical modeling of river ice processes. *Cold Regions Science and Technology*, *62*(1), 3–13. https://doi.org/10.1016/j.coldregions.2010.02.007

Turcotte, B., & Morse, B. (2013). A global river ice classification model. *Journal of Hydrology*, *507*, 134–148. https://doi.org/10.1016/j.jhydrol.2013.10.032

Walvoord, M. A., & Kurylyk, B. L. (2016). Hydrologic impacts of thawing permafrost—A review. *Vadose Zone Journal*, *15*(6), 1–20. https://doi.org/10.2136/vzj2016.01.0010

Walvoord, M. A., & Striegl, R. G. (2007). Increased groundwater to stream discharge from permafrost thawing in the Yukon River basin: Potential impacts on lateral export of carbon and nitrogen. *Geophysical Research Letters*, *34*(12). https://doi.org/10.1029/2007gl030216

Wilson, N. J., Walter, M. T., & Waterhouse, J. (2015). Indigenous knowledge of hydrologic change in the Yukon River basin: A case study of Ruby, Alaska. *Arctic*, *68*(1), 93–106. https://doi.org/10.14430/arctic4459

Wirth, L., Rosenberger, A., Prakash, A., Gens, R., Margraf, F. J., & Hamazaki, T. (2012). A remote-sensing, GIS-based approach to identify, characterize, and model spawning habitat for fall-run chum salmon in a sub-Arctic, glacially fed river. *Transactions of the American Fisheries Society*, *141*(5), 1349–1363. https://doi.org/10.1080/00028487.2012.692348

Yang, X., Pavelsky, T. M., & Allen, G. H. (2020). The past and future of global river ice. *Nature*, *577*(7788), 69–73. https://doi.org/10.1038/s41586-019-1848-1